5. Coastal dikes and embankment seawalls

5.1 Introduction

An exact mathematical description of the wave run-up and wave overtopping process for coastal dikes or embankment seawalls is not possible due to the stochastic nature of wave breaking and wave run-up and the various factors influencing the wave run-up and wave overtopping process. Therefore, wave run-up and wave overtopping for coastal dikes and embankment seawalls are mainly determined by empirical formulas derived from experimental investigations. The influence of roughness elements, wave walls, berms, etc. is taken into account by introducing influence factors. Thus, the following chapter is structured as follows.
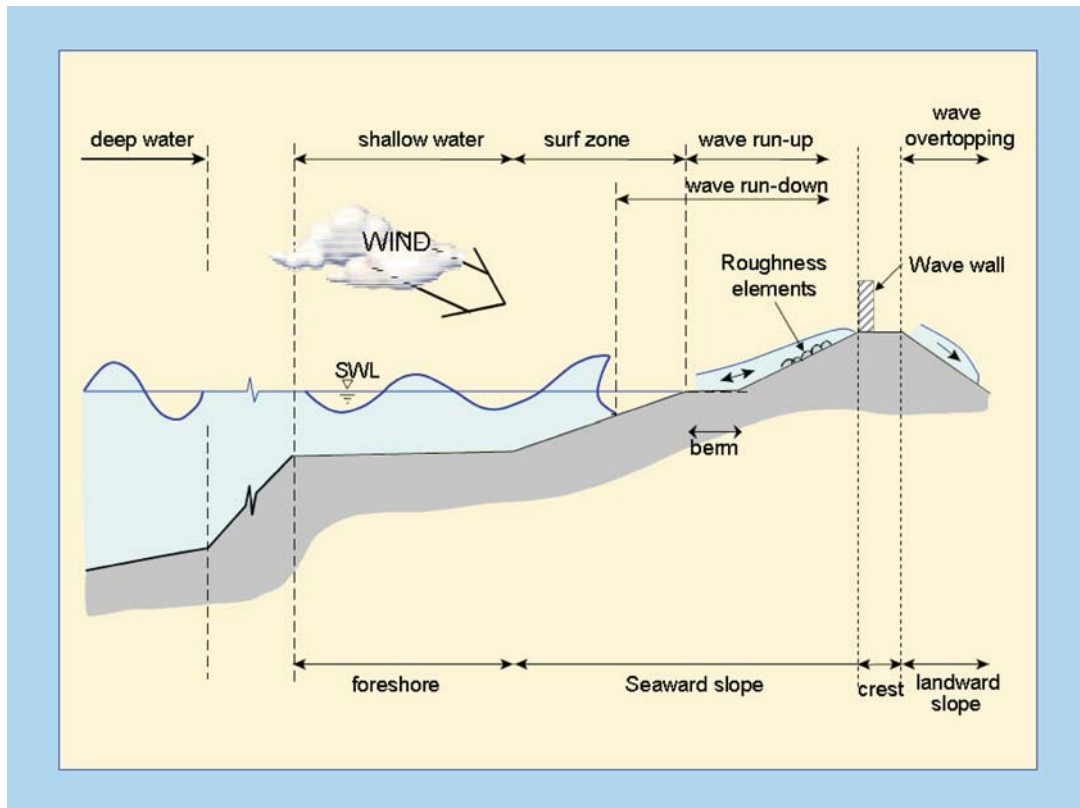

Fig. 5.1: Wave run-up and wave overtopping for coastal dikes and embankment seawalls: definition sketch. See Section 1.4 for definitions

First, wave run-up will be described as a function of the wave breaking process on the seaward slope for simple smooth and straight slopes. Then, wave overtopping is discussed with respect to average overtopping discharges and individual overtopping volumes. The influencing factors on wave run-up and wave overtopping like berms, roughness elements, wave walls and oblique wave attack are handled in the following section. Finally, the overtopping flow depth and the overtopping flow velocities are discussed as the direct influencing parameters to the surface of the structure. The main calculation procedure for coastal dikes and embankment seawalls is given in Fig. 5.2.

Simple slopes and conditions	Determinstic design	Probabilistic design
Wave run-up height	Eq. 5.4	Eq. 5.3
Mean overtopping discharge	Eq. 5.9	Eq. 5.8
Mean overtopping discharge (shallow foreshore)	Eq. 5.10	Eq. 5.11
Individual overtopping volumes	Eq. 5.35	Eq. 5.35
Complex slopes and conditions		
Effect of surface roughness	Table 5.2	Table 5.2
Effect of oblique waves	Eq. 5.23 for wave run-up	Eq. 5.23 for wave run-up
	Eq. 5.24 for wave overtopping	Eq. 5.24 for wave overtopping
Effect of composite slopes	Eq. 5.26	Eq. 5.26
Effect of berms	Eq. 5.27	Eq. 5.27
Effect of wave wall	Eq. 5.34	Eq. 5.34
Overtopping Flow Parameters	**Flow depth**	**Flow velocity**
Seaward slope	5.41	5.43
Dike crest	5.44	5.45
Landward slope	5.44	5.49

Fig. 5.2: Main calculation procedure for coastal dikes and embankment seawalls

Definitions of, and detailed descriptions of, wave run-up, wave overtopping, foreshore, structure, slope, berm and crest height are given in Section 1.4 and are not repeated here.

5.2 Wave run-up

The wave run-up height is defined as the vertical difference between the highest point of wave run-up and the still water level (SWL) (Fig. 5.3). Due to the stochastic nature of the incoming waves, each wave will give a different run-up level. In the Netherlands as well as in Germany many dike heights have been designed to a wave run-up height $R_{u2\%}$. This is the wave run-up height which is exceeded by 2 % of the number of incoming waves at the toe of the structure. The idea behind this was that if only 2 % of the waves reach the crest of a dike or embankment during design conditions, the crest and inner slope do not need specific protection measures other than clay with grass. It is for this reason that much research in the past has been focused on the 2%-wave run-up height. In the past decade the design or safety assessment has been changed to allowable overtopping instead of wave run-up. Still a good prediction of wave run-up is valuable as it is the basic input for calculation of number of overtopping waves over a dike, which is required to calculate overtopping volumes, overtopping velocities and flow depths.

The general formula that can be applied for the 2%-wave run-up height is given by Equation 5.1: The relative wave run-up height $R_{u,2\%}/H_{m0}$ in Equation 5.11 is related to the breaker parameter $\xi_{m-1,0}$. The breaker parameter or surf similarity parameter $\xi_{m-1,0}$ relates the slope steepness $\tan \alpha$ (or $1/n$) to the wave steepness $s_{m-1,0} = H_{m0}/L_0$ and is often used to distinguish different breaker types, see Section 1.4.

$$\frac{R_{u2\%}}{H_{m0}} = c_1 \cdot \gamma_b \cdot \gamma_f \cdot \gamma_\beta \cdot \xi_{m-1,0} \quad \text{with a maximum of} \quad \frac{R_{u2\%}}{H_{m0}} = \gamma_f \cdot \gamma_\beta \left(c_2 - \frac{c_3}{\sqrt{\xi_{m-1,0}}} \right)$$

where:

$R_{u2\%}$ = wave run-up height exceeded by 2 % of the incoming waves [m]

c_1, c_2 and c_3 = empirical coefficients [-] with   5.1
γ_b = influence factor for a berm [-]
γ_f = influence factor for roughness elements on a slope [-]
γ_β = influence factor for oblique wave attack [-]
$\xi_{m-1,0}$ = breaker parameter = $\tan\alpha/(s_{m-1,0})^{0.5}$ [-]
ξ_{tr} = transition breaker parameter between breaking and non-breaking waves (refer to Section 1.4.3)

The relative wave run-up height increases linearly with increasing $\xi_{m-1,0}$ in the range of breaking waves and small breaker parameters less than ξ_{tr}. For non-breaking waves and higher breaker parameter than ξ_{tr} the increase is less steep as shown in Fig. 5.4 and becomes more or less horizontal. The relative wave run-up height $R_{u,2\%}/H_{m0}$ is also influenced by: the geometry of the coastal dike or embankment seawall; the effect of wind; and the properties of the incoming waves.
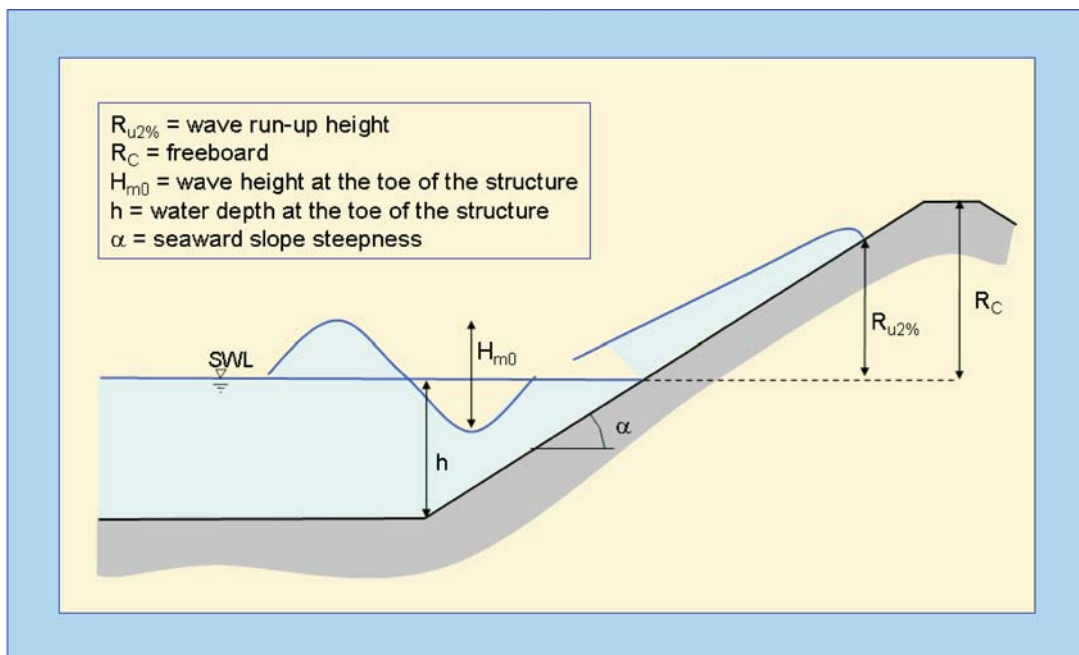

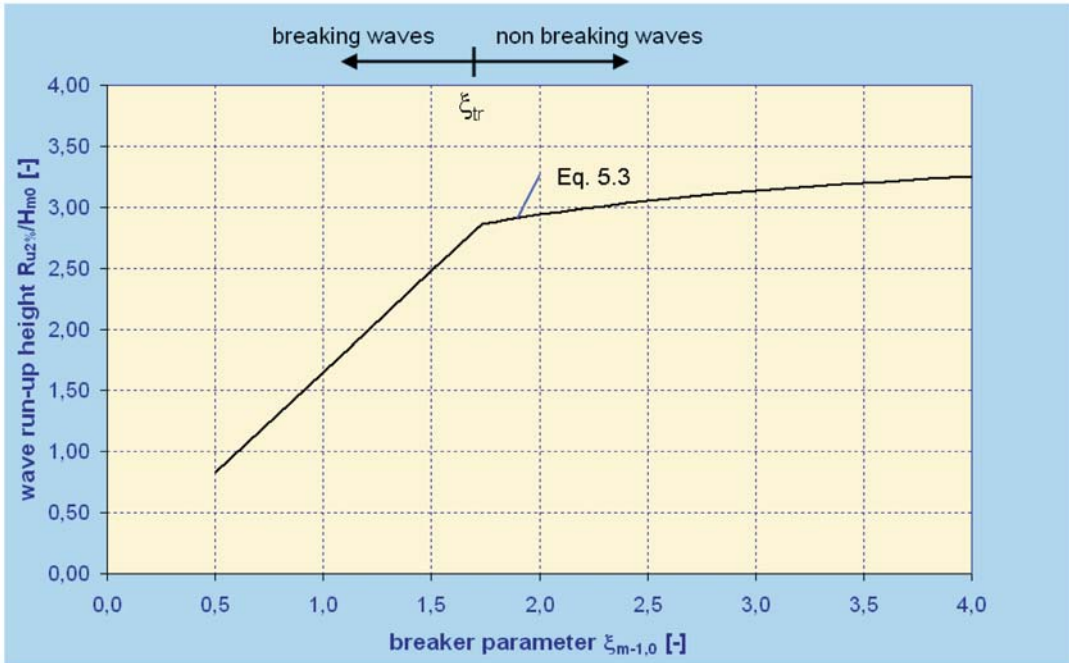Fig. 5.3: Definition of the wave run-up height $R_{u2\%}$ on a smooth impermeable slope

Fig. 5.4: Relative Wave run-up height $R_{u2\%}/H_{m0}$ as a function of the breaker parameter $\xi_{m-1,0}$, for smooth straight slopes
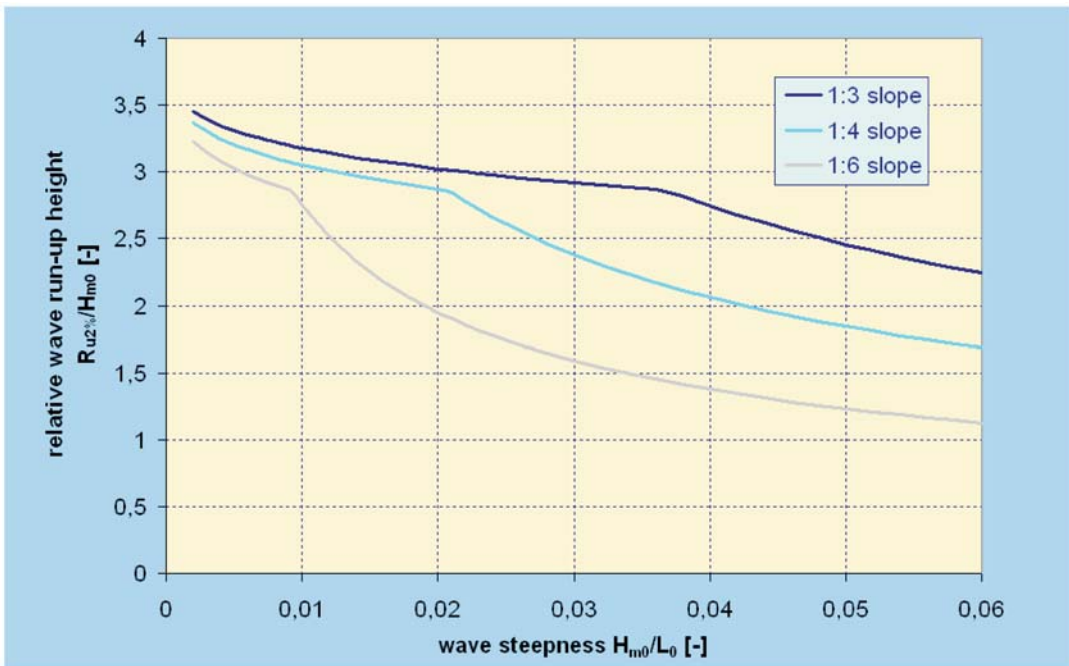

Fig. 5.5: Relative Wave run-up height $R_{u2\%}/H_{m0}$ as a function of the wave steepness for smooth straight slopes

The geometry of the coastal dike is considered by the slope tan α, the influence factor for a berm γ_b, the influence factor for a wave wall γ_V and the influence factor for roughness elements on the slope γ_f. These factors will be discussed in Sections 5.3.2, 5.3.4 and 5.3.5.

The effect of wind on the wave run-up-height for smooth impermeable slopes will mainly be focused on the thin layer in the upper part of the run-up. As described in Section 1.4, very thin layers of wave run-up are not considered and the run-up height was defined where the run-up layer becomes less than 1–2 cm. Wind will not have a lot of effect then. This was also proven in the European programme OPTICREST, where wave run-up on an actual smooth dike was compared with small scale laboratory measurements. Scale and wind effects were not found in those tests. It is recommended not to consider the influence of wind on wave run-up for coastal dikes or embankment seawalls.

The properties of the incoming waves are considered in the breaker parameter $\xi_{m-1,0}$ and the influence factor for oblique wave attack γ_β which is discussed in Section 5.3.3. As given in Section 1.4, the spectral wave period $T_{m-1,0}$ is most suitable for the calculation of the wave run-up height for complex spectral shapes as well as for theoretical wave spectra (JONSWAP, TMA, etc.). This spectral period $T_{m-1,0}$ gives more weight to the longer wave periods in the spectrum and is therefore well suited for all kind of wave spectra including bi-modal and multi-peak wave spectra. The peak period T_p, which was used in former investigations, is difficult to apply in the case of bi-modal spectra and should not be applied for multi peak or flat wave spectra as this may lead to large inaccuracies. Nevertheless, the peak period T_p is still in use for single peak wave spectra and there is a clear relationship between the spectral period $T_{m-1,0}$ and the peak period T_p for traditional single peak wave spectra:

$$T_p = 1.1 \ T_{m-1,0} \tag{5.2}$$

Similar relationships exist for theoretical wave spectra between $T_{m-1,0}$ and other period parameters like T_m and $T_{m0,1}$, see Section 1.4. As described in Section 1.4, it is recommended to use the spectral wave height H_{m0} for wave run-up height calculations.

The recommended formula for wave run-up height calculations is based on a large (international) dataset. Due to the large dataset for all kind of sloping structures a significant scatter is present, which cannot be neglected for application. There are several ways to include this uncertainty for application, but all are based on the formula describing the mean and a description of the uncertainty around this mean. This formula is given first and then three kinds of application: deterministic design or safety assessment; probabilistic design; and prediction or comparison with measurements. The formula is valid in the area of $0.5 < \gamma_b \cdot \xi_{m-1,0} \leq 8$ to 10.

The formula of wave run-up is given by Equation 5.3 and by the solid line in Fig. 5.6 which indicates the average value of the 2 % measured wave run-up heights.

$$\frac{R_{u2\%}}{H_{m0}} = 1.65 \cdot \gamma_b \cdot \gamma_f \cdot \gamma_\beta \cdot \xi_{m-1,0}$$

$$\text{with a maximum of } \frac{R_{u2\%}}{H_{m0}} = 1.00 \cdot \gamma_b \cdot \gamma_f \cdot \gamma_\beta \left(4.0 - \frac{1.5}{\sqrt{\xi_{m-1,0}}} \right) \tag{5.3}$$

Fig. 5.4 shows the influence of the wave steepness for different slopes on the dimensionless wave run-up height $R_{u2\%}/H_{m0}$.

The wave run-up formulas are given in Fig. 5.6 together with measured data from small and large scale model tests. All data were measured under perpendicular wave attack and in relatively deep water at the dike toe without any significant wave breaking in front of the dike toe.
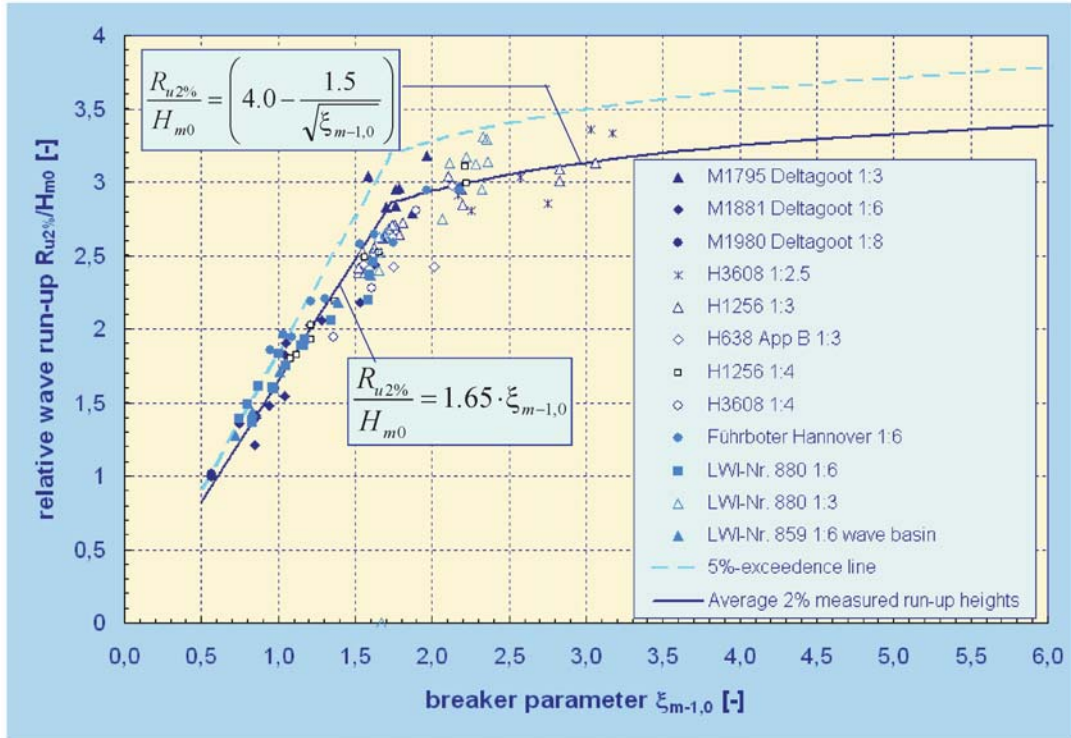

Fig. 5.6: Wave run-up for smooth and straight slopes

The statistical distribution around the average wave run-up height is described by a normal distribution with a variation coefficient $\sigma' = \sigma / \mu = 0.07$. It is this uncertainty which should be included in application of the formula. Exceedance lines, for example, can be drawn by using $R_{u2\%} / H_{m0} = \mu \pm x \cdot \sigma = \mu \pm x \cdot \sigma' \cdot \mu$, where μ is the prediction by Equation 5.3, $\sigma = \sigma' \cdot \mu$ the standard deviation, and x a factor of exceedance percentage according to the normal distribution. For example x = 1.64 for the 5 % exceedance limits and x = 1.96 for the 2.5 % exceedance limits. The 5 % upper exceedance limit is also given in Fig. 5.6.

$$\frac{R_{u2\%}}{H_{m0}} = 1.75 \cdot \gamma_b \cdot \gamma_f \cdot \gamma_\beta \cdot \xi_{m-1,0} \qquad \text{with a maximum of}$$

$$\frac{R_{u2\%}}{H_{m0}} = 1.00 \cdot \gamma_f \cdot \gamma_\beta \left(4.3 - \frac{1.6}{\sqrt{\xi_{m-1,0}}} \right)$$

5.4

Deterministic design or safety assessment: For design or a safety assessment of the crest height, it is advised not to follow the average trend, but to include the uncertainty of the prediction. In many international standards and guidelines a safety margin of about one standard deviation is used in formulae where the formula itself has significant scatter. Note

that this standard deviation does not take into account the uncertainty of the parameters used, like the wave height and period. The equation for deterministic calculations is given by the dashed line in Fig. 5.7 together with the equation for probabilistic design. Equation 5.4 is recommended for deterministic calculations.
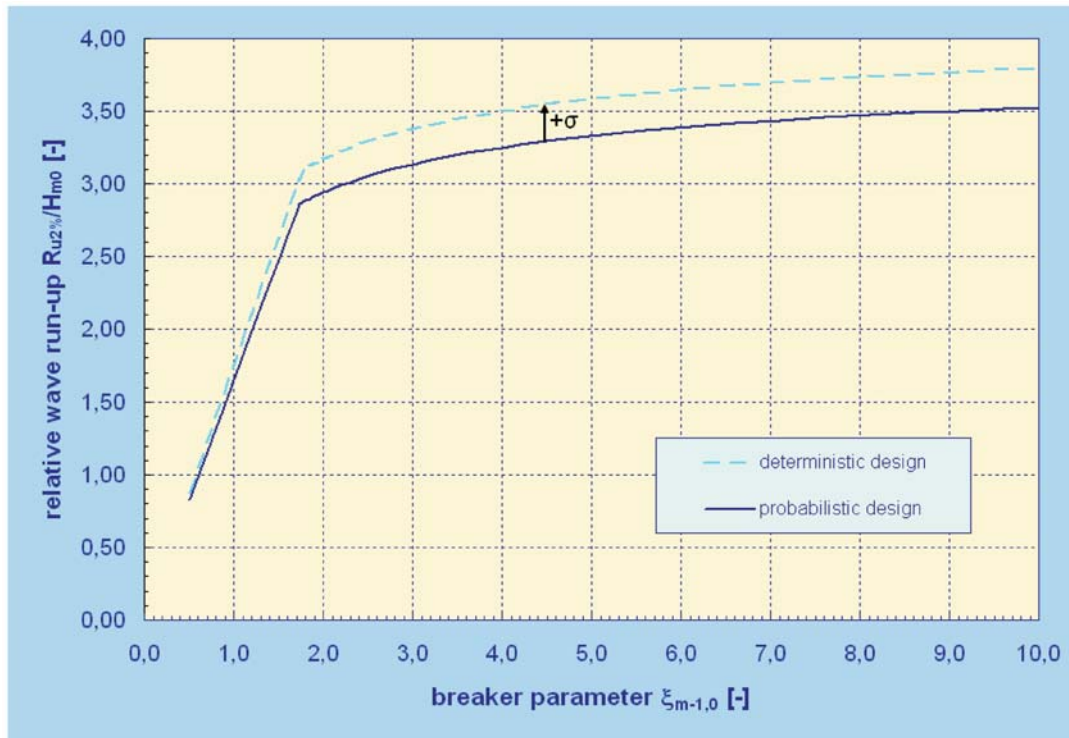

Fig. 5.7: Wave run-up for deterministic and probabilistic design

Probabilistic design: Besides deterministic calculations, probabilistic calculations can be made to include the effect of uncertainties of all parameters or to find optimum levels including the wind, wave and surge statistics. For probabilistic calculations Equation 5.3 is used together with the normal distribution and variation coefficient of $\sigma' = 0.07$.

Prediction or comparison of measurements: The wave run-up equation can also be used to predict a measurement in a laboratory (or in real situations) or to compare with measurements performed. In that case Equation 5.3 for the average wave run-up height should be used, preferably with for instance the 5 % upper and lower exceedance lines.

The influence factors γ_b, γ_f and γ_β where derived from experimental investigations. A combination of influence factors is often required in practice which reduces wave run-up and wave overtopping significantly. Systematic investigations on the combined influence of wave obliquity and berms showed that both influence factors can be used independently without any interactions. Nevertheless, a systematic combination over the range of all influence factors and all combinations was not possible until now. Therefore, further research is recommended if the overall influence factor $\gamma_b \gamma_f \gamma_\beta$ becomes lower than 0.4.

5.2.1 History of the 2% value for wave run-up

The choice for 2% has been made long ago and was probably arbitrary. The first international paper on wave run-up, mentioning the 2 % wave run-up, is ASBECK et al., 1953. The formula $R_{u2\%} = 8\ H_{m0}$ tanα has been mentioned there (for 5 % wave steepness and gentle smooth slopes, and this formula has been used for the design of dikes till 1980. But the choice for the 2 % was already made there.

The origin stems from the closing of the Southern Sea in the Netherlands in 1932 by the construction of a 32 km long dike (Afsluitdijk). This created the fresh water lake IJsselmeer and in the 45 years after closure about half of the lake was reclaimed as new land, called polders. The dikes for the first reclamation (North East Polder) had to be designed in 1936/1937. It is for this reason that in 1935 en 1936 a new wind-wave flume was built at Delft Hydraulics and first tests on wave run-up were performed in 1936. The final report on measurements (report M101), however, was issued in 1941 "due to lack of time". But the measurements had been analysed in 1936 to such a degree that "the dimensions of the dikes of the North East Polder could be established". That report could not be retrieved from Delft Hydraulics' library. The M101 report gives only the 2 % wave run-up value and this must have been the time that this value would be the right one to design the crest height of dikes.

Further tests from 1939–1941 on wave run-up, published in report M151 in 1941, however, used only the 1% wave run-up value. Other and later tests (M422, 1953; M500, 1956 and M544, 1957) report the 2% value, but for completeness give also the 1 %, 10 %, 20 % and 50 %.

It can be concluded that the choice for the 2% value was made in 1936, but the reason why is not clear as the design report itself could not be retrieved.

5.3 Wave overtopping discharges

5.3.1 Simple slopes

Wave overtopping occurs if the crest level of the dike or embankment seawall is lower than the highest wave run-up level R_{max}. In that case, the freeboard RC defined as the vertical difference between the still water level (SWL) and the crest height becomes important (Fig. 5.3). Wave overtopping depends on the freeboard RC and increases for decreasing freeboard height RC. Usually wave overtopping for dikes or coastal embankments is described by an average wave overtopping discharge q, which is given in m³/s per m width, or in litres/s per m width.

An average overtopping discharge q can only be calculated for quasi-stationary wave and water level conditions. If the amount of water overtopping a structure during a storm is required, the average overtopping discharge has to be calculated for each more or less constant storm water level and constant wave conditions.

Many model studies were performed to investigate the average overtopping discharge for specific dike geometries or wave conditions. For practical purposes, empirical formulae were fitted through experimental model data which obey often one of the following expressions:

$$Q_* = Q_0\ (1 - R_*)^b \quad \text{or} \quad Q_* = Q_0 \exp(-\ b \cdot R_*) \qquad 5.5$$

Q_* is a dimensionless overtopping discharge, R_* is a dimensionless freeboard height, Q_0 describes wave overtopping for zero freeboard and b is a coefficient which describes the specific behaviour of wave overtopping for a certain structure. SCHÜTTRUMPF (2001) summarised expressions for the dimensionless overtopping discharge Q_* and the dimensionless freeboard height R_*.

As mentioned before, the average wave overtopping discharge q depends on the ratio between the freeboard height R_C and the wave run-up height R_u:

$$\frac{R_C}{R_u} \qquad\qquad 5.6$$

The wave run-up height R_u can be written in a similar expression as the wave run-up height $R_{u,2\%}$ giving the following relative freeboard height:

$$\frac{R_C}{c_{u,1} \cdot \xi_{m-1,0} \cdot H_{m0} \cdot \gamma_b \cdot \gamma_f \cdot \gamma_\beta \cdot \gamma_v} \quad \text{for breaking waves and a maximum of}$$

$$\qquad\qquad 5.7$$

$$\frac{R_C}{c_{u,2} \cdot H_{m0} \cdot \gamma_f \cdot \gamma_\beta} \quad \text{for non-breaking waves}$$

The relative freeboard does not depend on the breaker parameter $\xi_{m-1,0}$ for non breaking waves (Fig. 5.8), as the line is horizontal.
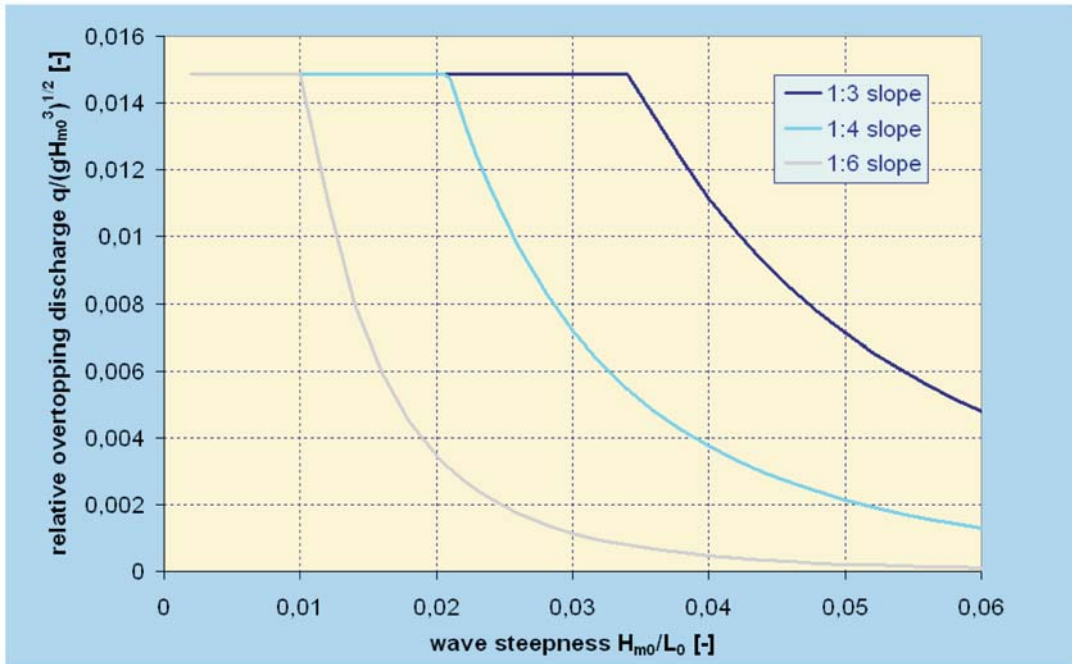

Fig. 5.8: Wave overtopping as a function of the wave steepness H_{m0}/L_0 and the slope

The dimensionless overtopping discharge $Q^* = q/(gH^3_{m0})^{1/2}$ is a function of the wave height, originally derived from the weir formula.

Probabilistic design and prediction or comparison of measurements ($\xi_{m-1,0}<5$): TAW (2002) used these dimensionless factors to derive the following overtopping formulae for breaking and non-breaking waves, which describe the *average* overtopping discharge:

$$\frac{q}{\sqrt{g \cdot H_{m0}^3}} = \frac{0.067}{\sqrt{\tan\alpha}} \gamma_b \cdot \xi_{m-1,0} \cdot \exp\left(-4.75 \frac{R_C}{\xi_{m-1,0} \cdot H_{m0} \cdot \gamma_b \cdot \gamma_f \cdot \gamma_\beta \cdot \gamma_v} \right)$$

$$\text{with a maximum of: } \frac{q}{\sqrt{g \cdot H_{m0}^3}} = 0.2 \cdot \exp\left(-2.6 \frac{R_C}{H_{m0} \cdot \gamma_f \cdot \gamma_\beta} \right)$$

5.8

The reliability of Equation 5.8 is described by taking the coefficients 4.75 and 2.6 as normally distributed stochastic parameters with means of 4.75 and 2.6 and standard deviations $\sigma = 0.5$ and 0.35 respectively. For probabilistic calculations Equation 5.8 should be taken together with these stochastic coefficients. For predictions of measurements or comparison with measurements also Equation 5.8 should be taken with, for instance, 5 % upper and lower exceedance curves.

Equation 5.8 is given in Fig. 5.9 together with measured data for breaking waves from different model tests in small and large scale as well as in wave flumes and wave basins. In addition, the 5 % lower and upper confidence limits are plotted.
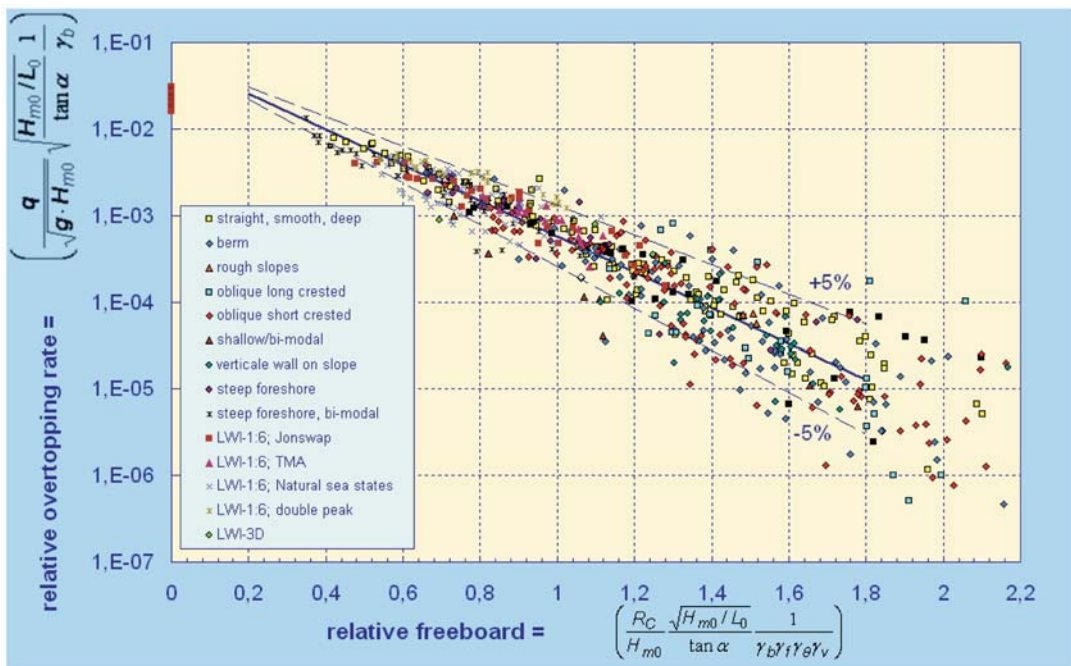

Fig. 5.9: Wave overtopping data for breaking waves and overtopping Equation 5.8 with 5 % under and upper exceedance limits

Data for non-breaking waves are presented in Fig. 5.10 together with measured data, the overtopping formula for non-breaking waves and the 5 % lower and upper confidence limits.

Equation 5.8 gives the averages of the measured data and can be used for probabilistic calculations or predictions and comparisons with measurements.

Deterministic design or safety assessment ($\xi_{m-1,0}$<5): For deterministic calculations in design or safety assessment it is strongly recommended to increase the average discharge by about one standard deviation. Thus, Equation 5.9 should be used for deterministic calculations in design and safety assessment:

$$\frac{q}{\sqrt{g \cdot H_{m0}^3}} = \frac{0.067}{\sqrt{\tan\alpha}} \gamma_b \cdot \xi_{m-1,0} \cdot \exp\left(-4.3 \frac{R_C}{\xi_{m-1,0} \cdot H_{m0} \cdot \gamma_b \cdot \gamma_f \cdot \gamma_\beta \cdot \gamma_v}\right)$$

$$\text{with a maximum of: } \frac{q}{\sqrt{g \cdot H_{m0}^3}} = 0.2 \cdot \exp\left(-2.3 \frac{R_C}{H_{m0} \cdot \gamma_f \cdot \gamma_\beta}\right)$$

5.9

A comparison of the two recommended formulas for deterministic design and safety assessment (Equation 5.8) and probabilistic calculations (Equation 5.9) for breaking and non-breaking waves is given in Fig. 5.11 and Fig. 5.12.

In the case of very heavy breaking on a shallow foreshore the wave spectrum is often transformed in a flat spectrum with no significant peak. In that case, long waves are present and influencing the breaker parameter $\xi_{m-1,0}$. Other wave overtopping formulas (equation 5.10 and 5.11) are recommended for shallow and very shallow foreshores to avoid a large
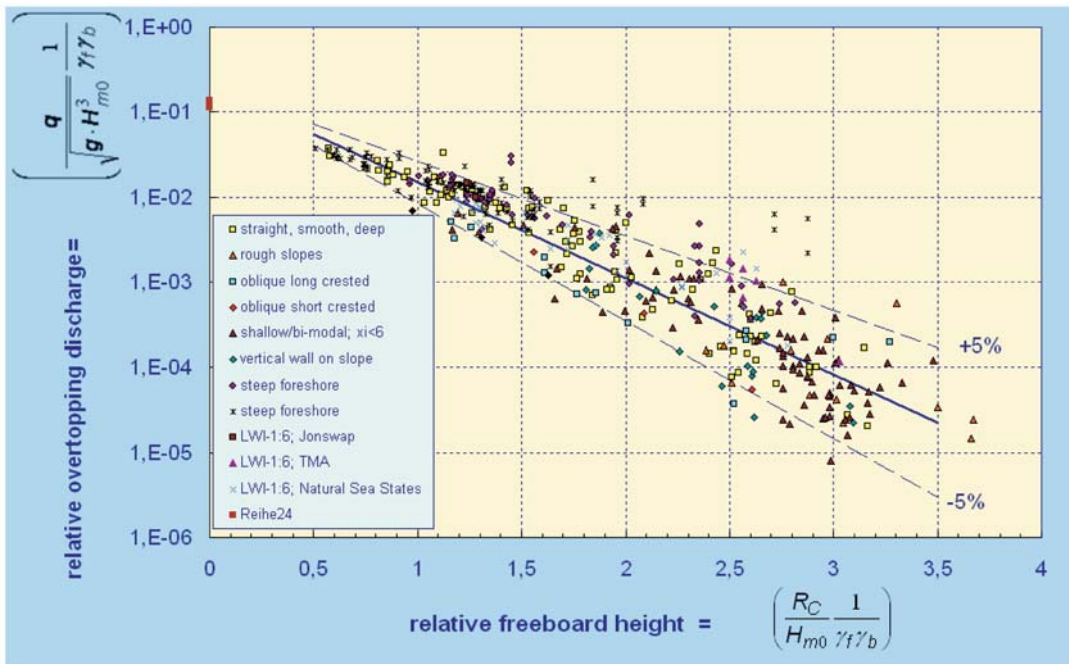

Fig. 5.10: Wave overtopping data for non-breaking waves and overtopping Equation 5.9 with 5 % under and upper exceedance limits
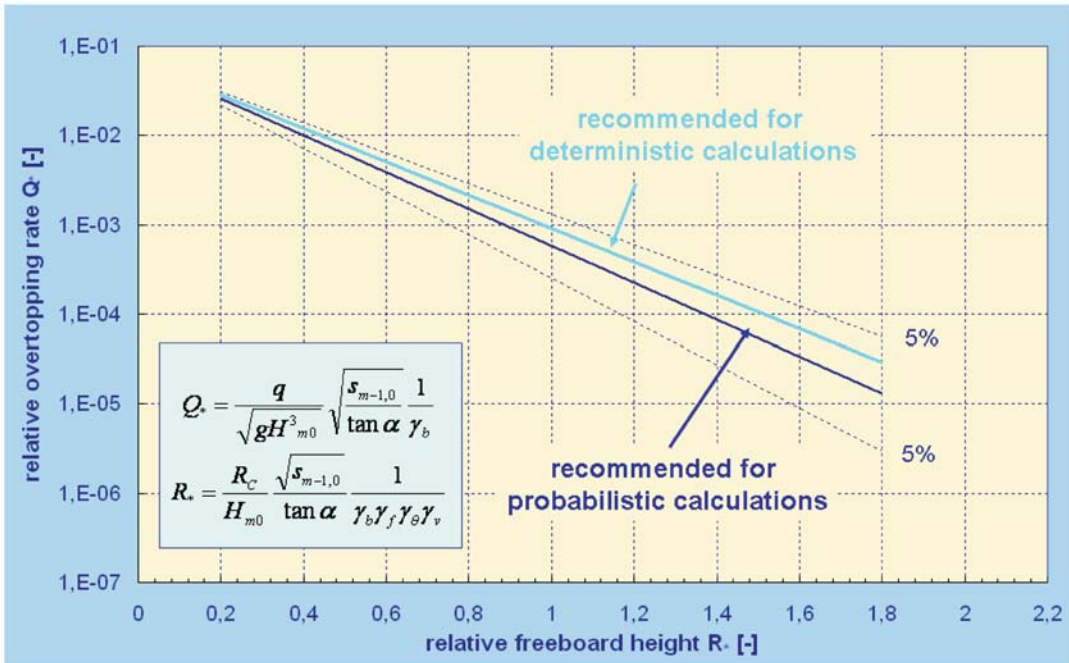
Fig. 5.11: Wave overtopping for breaking waves – Comparison of formulae for design and safety assessment and probabilistic calculations
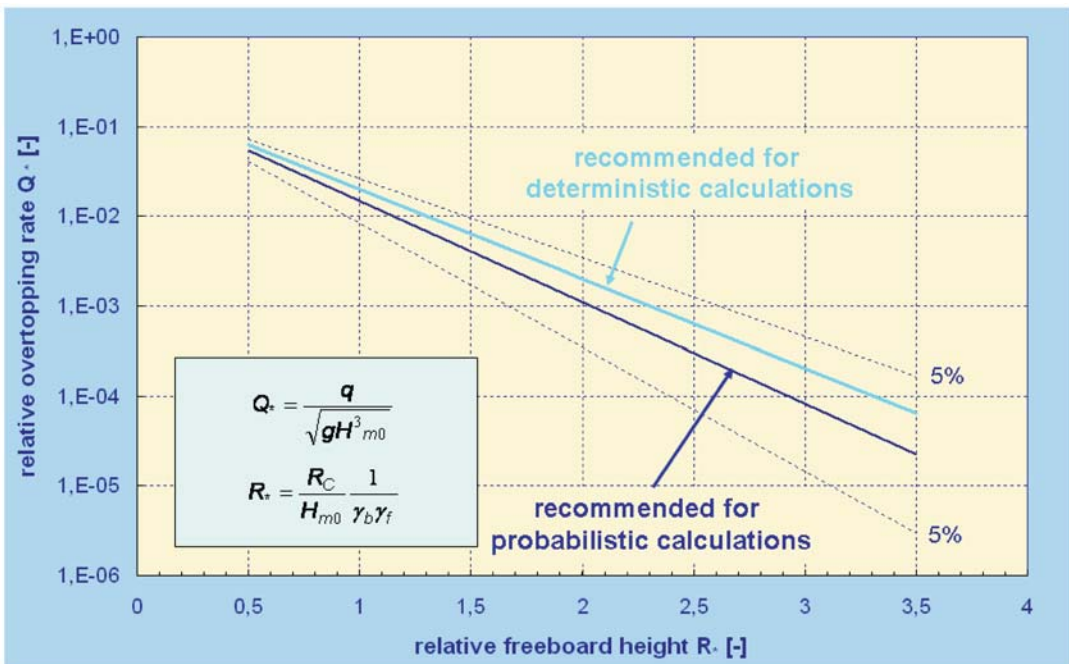

Fig. 5.12: Wave overtopping for non-breaking waves – Comparison of formulae for design and safety assessment and probabilistic calculations

underestimation of wave overtopping by using formulas 5.8 and 5.9. Since formulas 5.8 and 5.9 are valid for breaker parameters $\xi_{m-1,0}<5$ a linear interpolation is recommended for breaker parameters $5<\xi_{m-1,0}<7$.

Deterministic design or safety assessment ($\xi_{m-1,0}>7$): The following formula is recommended including a safety margin for deterministic design and safety assessment.

$$\frac{q}{\sqrt{g \cdot H_{m0}^3}} = 0.21 \cdot \exp\left(-\frac{R_C}{\gamma_f \cdot \gamma_\beta \cdot H_{m0} \cdot (0.33 + 0.022 \cdot \xi_{m-1,0})}\right) \qquad 5.10$$

Probabilistic design and prediction or comparison of measurements ($\xi_{m-1,0}>7$): The following formula was derived from measurements with a mean of –0.92 and a standard deviation of 0.24:

$$\frac{q}{\sqrt{g \cdot H_{m0}^3}} = 10^c \cdot \exp\left(-\frac{R_C}{\gamma_f \cdot \gamma_\beta \cdot H_{m0} \cdot (0.33 + 0.022 \cdot \xi_{m-1,0})}\right) \qquad 5.11$$

British guidelines recommend a slightly different formula to calculate wave overtopping for smooth slopes, which was originally developed by OWEN (1980) for smooth sloping and bermed seawalls:

$$\frac{q}{T_m \cdot g \cdot H_S} = Q_0 \cdot \exp\left(-b \cdot \frac{R_C}{T_m \sqrt{g \cdot H_S}}\right) \qquad 5.12$$

where Q_0 and b are empirically derived coefficients given in Table 5.1 (for straight slopes only).

Table 5.1: Owen's coefficients for simple slopes

Seawall Slope	Q_0	b
1:1	7.94E-3	20.1
1:1.5	8.84E-3	19.9
1:2	9.39E-3	21.6
1:2.5	1.03E-2	24.5
1:3	1.09E-2	28.7
1:3.5	1.12E-2	34.1
1:4	1.16E-2	41.0
1:4.5	1.20E-2	47.7
1:5	1.31E-2	55.6

Equation 5.2 uses the mean period T_m instead of the spectral wave period $T_{m-1,0}$ and has therefore the limitation of normal single peaked spectra which are not too wide or too narrow. Furthermore H_s, being $H_{1/3}$, was used and not H_{m0}, although this only makes a difference in shallow water. Equation 5.12 looks quite different to 5.8 and 5.9, but actually can be rewritten to a shape close to the breaking wave part of these formulae:

$$\frac{q}{\sqrt{g \cdot H_s^3}} = Q_0 / \sqrt{s_{0,m}} \cdot \exp\left(-b \frac{R_C}{H_s \sqrt{s_{0,m}}}\right) \qquad\qquad 5.13$$

If now tanα would be introduced in Equation 5.12 with a fit to the coefficients in Table 5.1, a similar formula as the breaking wave Equation 5.9 would be found. One restriction is that Equation 5.12 has no maximum for breaking waves, which may lead to significant over predictions for steep slopes and long waves.

The original data of OWEN (1980) were also used to develop Equations 5.8 and 5.9, which avoids the interpolation effort of the Owen formula for different slope angles given in Table 5.1 and overcomes other restrictions described above. But there is no reason not to use Equation 5.12 within the limits of application.

Zero Freeboard: Wave overtopping for zero freeboard (Fig. 5.13) becomes important if a dike or embankment seawall is overtopping resistant (for example a low dike of asphalt) and the water level comes close to the crest. SCHÜTTRUMPF (2001) performed model tests for different straight and smooth slopes in between 1:3 and 1:6 to investigate wave overtopping for zero freeboard and derived the following formula (σ' = 0.14), which should be used for probabilistic design and prediction and comparison of measurements (Fig. 5.14):

$$\frac{q}{\sqrt{g \cdot H_{m0}^3}} = 0.0537 \cdot \xi_{m-1,0} \qquad\qquad \text{for: } \xi_{m-1,0} < 2.0$$

$$\frac{q}{\sqrt{g \cdot H_{m0}^3}} = \left(0.136 - \frac{0.226}{\xi_{m-1,0}^3}\right) \qquad\qquad \text{for: } \xi_{m-1,0} \geq 2.0$$

$$5.14$$

For deterministic design or safety assessment it is recommended to increase the average overtopping discharge in Equation 5.14 by about one standard deviation.

Negative freeboard: If the water level is higher than the crest of the dike or embankment seawall, large overtopping quantities overflow/overtop the structure. In this situation, the amount of water flowing to the landward side of the structure is composed by a part which can be attributed to overflow ($q_{overflow}$) and a part which can be attributed to overtopping ($q_{overtop}$). The part of overflowing water can be calculated by the well known weir formula for a broad crested structure:

$$q_{overflow} = 0.6 \cdot \sqrt{g \cdot \left|- R_C^3\right|} \qquad\qquad 5.15$$

where R_C is the (negative) relative crest height and $-R_c$ is the overflow depth [m]

The effect of wave overtopping ($q_{overtop}$) is accounted for by the overtopping discharge at zero freeboard ($R_C = 0$) in Equation 5.14 as a first guess.

The effect of combined wave run-up and wave overtopping is given by the superposition of overflow and wave overtopping as a rough approximation:

$$q = q_{overflow} + q_{overtop} = 0.6 \cdot \sqrt{g \cdot \left|- R_C^3\right|} + 0.0537 \cdot \xi_{m-1,0} \cdot \sqrt{g \cdot H_{m0}^3}$$
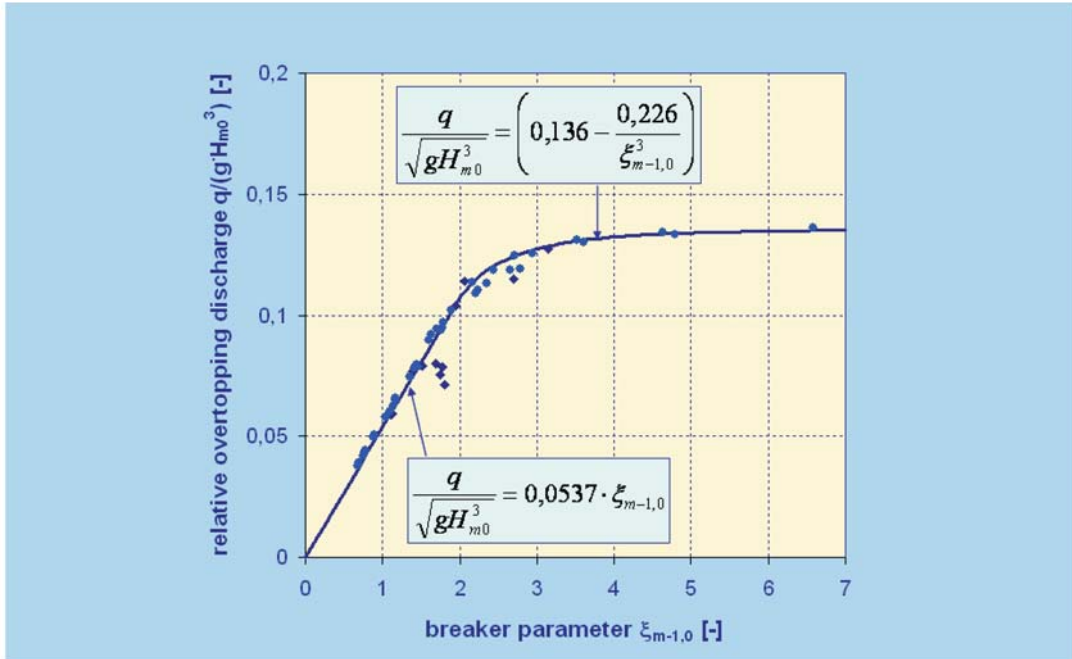$$\text{for: } \xi_{m-1,0} < 2.0 \qquad\qquad 5.16$$

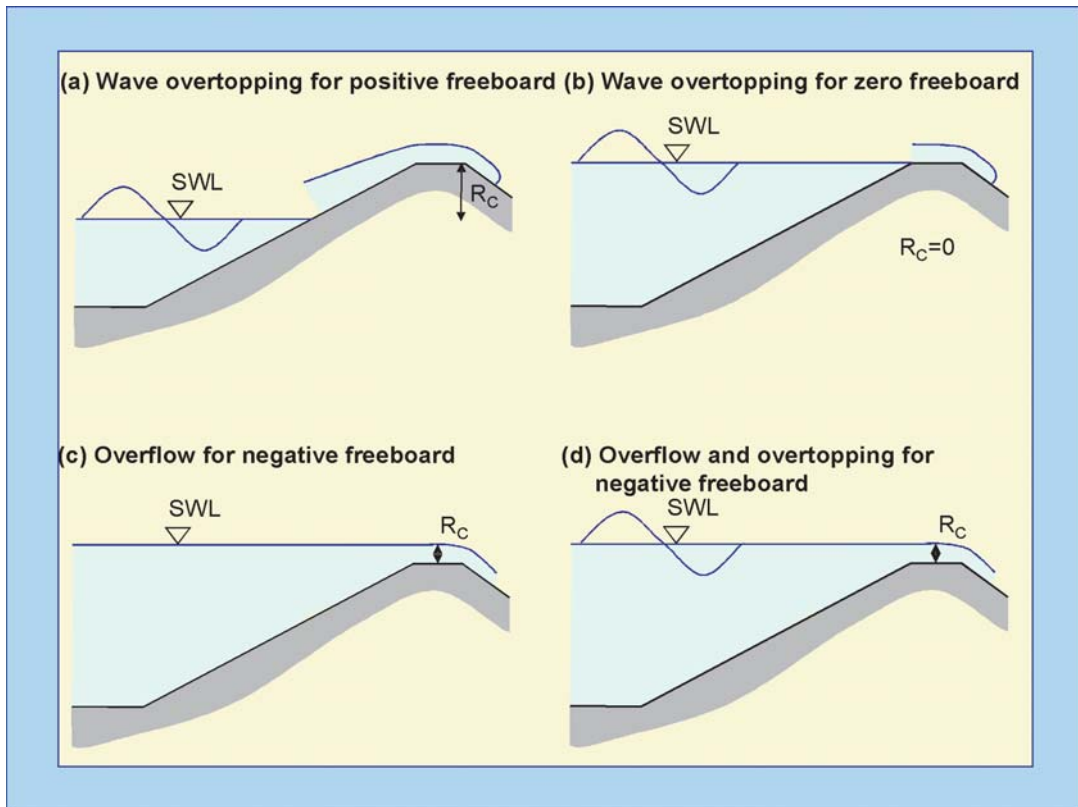Fig. 5.13: Dimensionless overtopping discharge for zero freeboard (SCHÜTTRUMPF, 2001)

Fig. 5.14: Wave overtopping and overflow for positive, zero and negative freeboard

Wave overtopping is getting less important for increasing overflow depth R_C. An experimental verification of Equation 5.16 is still missing. Therefore, no distinction was made here for probabilistic and deterministic design.

5.3.2   Effect of roughness

Most of the seadikes and embankment seawalls are on the seaward side covered either by grass (Fig. 5.15), by asphalt (Fig. 5.16) or by concrete or natural block revetment systems (Fig. 5.17). Therefore, these types of surface roughness (described as smooth slopes) were often used as reference in hydraulic model investigations and the influence factor for surface roughness γ_f of these smooth slopes for wave heights greater than about 0.75 m is equal to $\gamma_f = 1.0$.

Fig. 5.15: Dike covered by grass (photo: SCHÜTTRUMPF)

Fig. 5.16: Dike covered by asphalt (photo: SCHÜTTRUMPF)

Fig. 5.17: Dike covered by natural bloc revetment (photo: SCHÜTTRUMPF)

For significant wave heights H_s less than 0.75 m, grass influences the run-up process and lower influence factors γ_f are recommended by TAW (1997) (Fig. 5.18). This is due to the relatively greater hydraulic roughness of the grass surface for thin wave run-up depths.

$$\gamma_f = 1.15 \, H_S^{0.5} \text{ for grass and } H_S < 0.75 \text{ m} \qquad\qquad 5.17$$

Fig. 5.18: Influence factor for grass surface

Roughness elements (Fig. 5.19) or slopes partly covered by rock are often used to increase the surface roughness and to reduce the wave run-up height and the wave overtopping rate. Roughness elements are either used to influence the wave run-up or the wave run-down process. Fig. 5.21 shows the influence of artificial roughness elements on the wave run-up and run-down process. Roughness elements are applied either across the entire slope or for parts of the slope which should be considered during the calculation process.

Available data on the influence of surface roughness on wave run-up and wave overtopping are based on model tests in small, but mainly in large scale, in order to avoid scale effects. A summary of typical types of surface roughness is given in Table 5.2.

The influence factors for roughness elements apply for $\gamma_b \cdot \xi_{m-1,0} < 1.8$, increase linearly up to 1.0 for $\gamma_b \cdot \xi_{m-1,0} = 10$ and remain constant for greater values. The efficiency of artificial roughness elements such as blocks or ribs depends on the width of the block or rib f_b, the height of the blocks f_h and the distance between the ribs f_L. The optimal ratio between the height and the width of the blocks was found to be $f_h/f_b = 5$ to 8 and the optimal distance between ribs is $f_L/f_b = 7$. When the total surface is covered by blocks or ribs and when the height is at least $f_h/H_{m0} = 0.15$, then the following minimum influence factors are found:

Block, 1/25 of total surface covered	$\gamma_{f,min} = 0.85$
Block, 1/9 of total surface covered	$\gamma_{f,min} = 0.80$
Ribs, $f_L/f_b = 7$ apart (optimal)	$\gamma_{f,min} = 0.75$

Fig. 5.19: Example for roughness elements (photo: SCHÜTTRUMPF)

Table 5.2: Surface roughness factors for typical elements

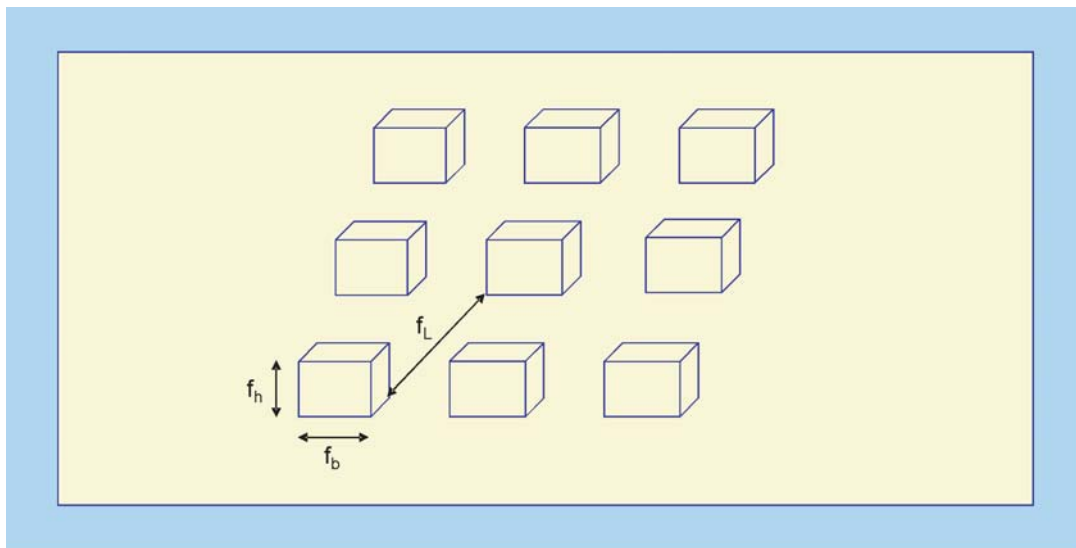| Reference type	γ_f
Concrete	1.0
Asphalt	1.0
Closed concrete blocks	1.0
Grass	1.0
Basalt	0.90
Small blocks over 1/25 of surface	0.85
Small blocks over 1/9 of surface	0.80
¼ of stone setting 10 cm higher	0.90
Ribs (optimum dimensions)	0.75

Fig. 5.20: Dimensions of roughness elements

A greater block or rib height than $f_h/H_{m0} = 0.15$ has no further reducing effect. If the height is less, then an interpolation is required:

$$\gamma_f = 1 - (1 - \gamma_{f,\,min}) \cdot \left(\frac{f_h}{0.15 \cdot H_{m0}} \right) \quad \text{for: } f_h/H_{m0} < 0.15 \qquad 5.18$$

As already mentioned, roughness elements are mostly applied for parts of the slope. Therefore, a reduction factor is required which takes only this part of the slope into account.

It can be shown that roughness elements have no or little effect below $0.25 \cdot R_{u2\%,smooth}$ below the still water line and above $0.50 \cdot R_{u2\%,smooth}$ above the still water line. The resulting influence factor γ_f is calculated by weighting the various influence factors $\gamma_{f,i}$ and by including the lengths L_i of the appropriate sections i in between SWL-$0.25 \cdot R_{u2\%smooth}$ and SWL + $0.50 \cdot R_{u2\%smooth}$:

$$\gamma_f = \frac{\sum_{i=1}^{n} \gamma_{f,i} \cdot L_i}{\sum_{i=1}^{n} L_i} \qquad 5.19$$

It appears that roughness elements applied only under water (with a smooth upper slope) have no effect and, in such a case, should be considered as a smooth slope. For construction purposes, it is recommended to restrict roughness elements to their area of influence. The construction costs will be less than covering the entire slope by roughness elements.

The effect of roughness elements on wave run-up may be reduced by debris between the elements.

Fig. 5.21: Performance of roughness elements showing the degree of turbulence

5.3.3 Effect of oblique waves

Wave run-up and wave overtopping can be assumed to be equally distributed along the longitudinal axis of a dike. If this axis is curved, wave run-up or wave overtopping will certainly increase for concave curves; with respect to the seaward face; due to the accumulation of wave run-up energy. Similarly, wave run-up and overtopping will decrease for convex curves, due to the distribution of wave run-up energy. No experimental investigations are known concerning the influence of a curved dike axis and the spatial distribution of wave run-up and wave overtopping yet.

Only limited research is available on the influence of oblique wave attack on wave run-up and wave overtopping due to the complexity and the high costs of model tests in wave basins. Most of the relevant research was performed on the influence of long crested waves and only few investigations are available on the influence of short crested waves on wave run-up and wave overtopping. Long crested waves have no directional distribution and wave crests are parallel and of infinite width. Only swell coming from the ocean can be regarded as a long crested wave. In nature, storm waves are short crested (Fig. 5.23). This means, that wave crests are not parallel, the direction of the individual waves is scattered around the main direction and the crests of the waves have a finite width. The directional spreading might be characterized by the directional spreading width σ or the spreading factor s. Relations between these parameters are approximately:

$$ s = \frac{2 - \sigma^2}{\sigma^2} \text{ or: } \sigma = \sqrt{\frac{2}{s+1}} \qquad\qquad 5.20 $$

The directional spreading width is σ = 0° (s = ∞) for long crested waves. Results of systematic research on the influence of oblique wave attack on wave run-up and wave overtopping under short crested wave conditions are summarized in EAK (2002) and TAW (2002). The data of this systematic research were summarized in Fig. 5.24. Data for long crested waves are not presented here.

The angle of wave attack β is defined at the toe of the structure after any transformation on the foreshore by refraction or diffraction as the angle between the direction of the waves and the perpendicular to the long axis of the dike or revetment as shown in Fig. 5.22. Thus, the direction of wave crests approaching parallel to the dike axis is defined as β = 0° (perpen-

dicular wave attack). The influence of the wave direction on wave run-up or wave overtopping is defined by an influence factor γ_β:

$$\gamma_\beta = \frac{R_{u2\%;\beta>0°}}{R_{u2\%;\beta=0°}} \text{ for wave run-up} \qquad\qquad 5.21$$

$$\gamma_\beta = \frac{q_{\beta>0°}}{q_{\beta=0°}} \text{ for wave overtopping} \qquad\qquad 5.22$$

For practical purposes, it is recommended to use the following expressions for short crested waves to calculate the influence factor γ_β for wave run-up:

$$\gamma_\beta = 1 - 0.0022|\beta| \text{ for} : 0° \leq \beta \leq 80°$$
$$\gamma_\beta = 0.824 \text{ for} : |\beta| > 80° \qquad\qquad 5.23$$

and wave overtopping

$$\gamma_\beta = 1 - 0.0033|\beta| \text{ for} : 0° \leq \beta \leq 80°$$
$$\gamma_\beta = 0.736 \text{ for} : |\beta| > 80° \qquad\qquad 5.24$$

New model tests (SCHÜTTRUMPF et al. (2003)) indicate that formulae 5.21 and 5.22 overestimate slightly the reduction of wave run-up and wave overtopping for small angles of wave attack. The influence of wave direction on wave run-up or wave overtopping can be even neglected for wave directions less than $|\beta| = 20°$.

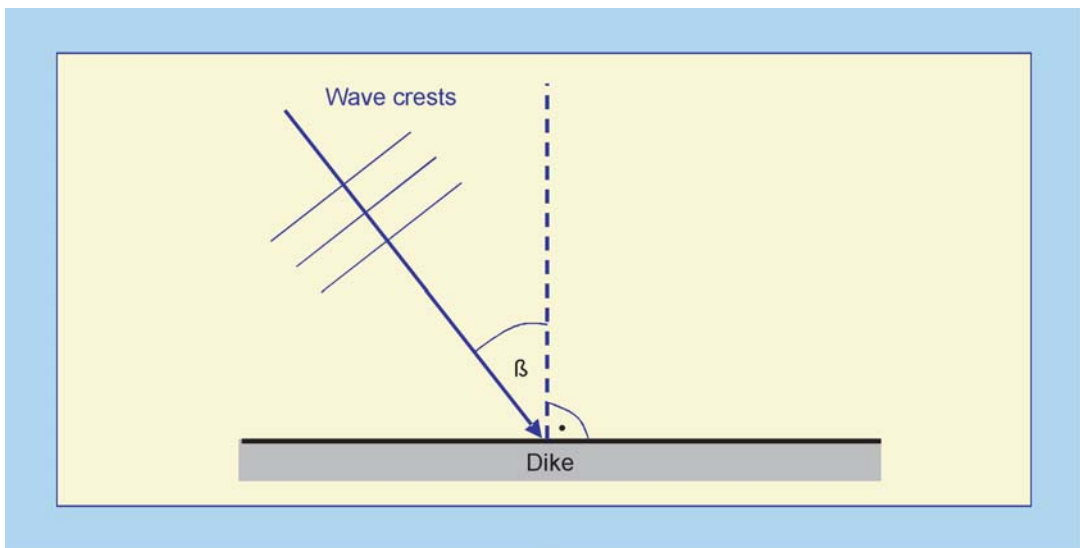Fig. 5.22: Definition of angle of wave attack β

Fig. 5.23: Short crested waves resulting in wave run-up and wave overtopping (photo: ZITSCHER)

For wave directions $80° < |\beta| \leq 110°$ waves are diffracted around the structure and an adjustment of the wave height H_{m0} and the wave period $T_{m-1,0}$ are recommended:

$$H_{m0} \text{ is multiplied by } \frac{110 - |\beta|}{30} \qquad T_{m-1,0} \text{ is multiplied by } \sqrt{\frac{110 - |\beta|}{30}}$$

For wave directions between $110° < |\beta| \leq 180°$ wave run-up and wave overtopping are set to $R_{u2\%} = 0$ and $q = 0$.

No significant influence of different spreading widths s (s = ∞, 65, 15 and 6) was found in model tests. As long as some spreading is present, short-crested waves behave similar independent of the spreading width. The main point is that short-crested oblique waves give different wave run-up and wave overtopping than long-crested waves.
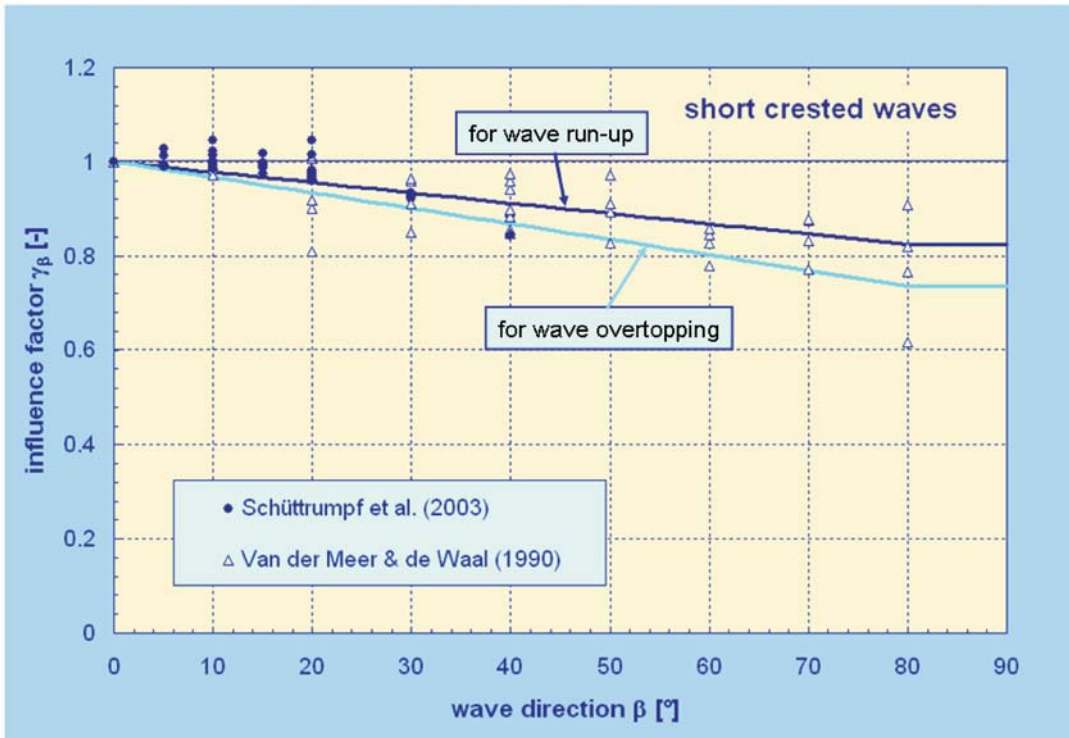
Fig. 5.24: Influence factor γ_β for oblique wave attack and short crested waves, measured data are for wave run-up

5.3.4 Composite slopes and berms

(a) Average slopes: Many dikes do not have a straight slope from the toe to the crest but consist of a composite profile with different slopes, a berm or multiple berms. A character-istic slope is required to be used in the breaker parameter $\xi_{m-1,0}$ for composite profiles or bermed profiles to calculate wave run-up or wave overtopping. Theoretically, the run-up process is influenced by a change of slope from the breaking point to the maximum wave run-up height. Therefore, often it has been recommended to calculate the characteristic slope from the point of wave breaking to the maximum wave run-up height. This approach needs some calculation effort, because of the iterative solution since the wave run-up height $R_{u2\%}$ is unknown. For the breaking limit a point on the slope can be chosen which is $1.5\,H_{m0}$ below the still water line.

It is recommended to use also a point on the slope $1.5\,H_{m0}$ above water as a first estimate to calculate the characteristic slope and to exclude a berm (Fig. 5.25).

$$1^{st}\ \text{estimate:}\ \ \tan\alpha = \frac{3 \cdot H_{m0}}{L_{Slope} - B} \qquad\qquad 5.25$$

As a second estimate, the wave run-up height from the first estimate is used to calculate the average slope (L_{Slope} has to be adapted see Fig. 5.26):
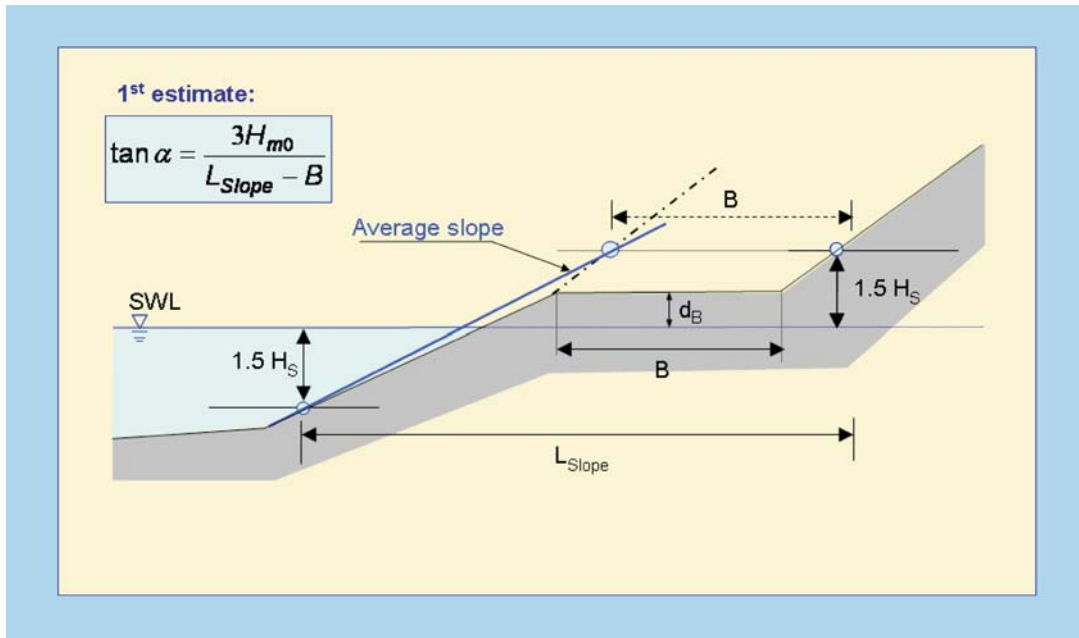
Fig. 5.25: Determination of the average slope (1st estimate)

$$2^{\text{nd}} \text{ estimate: } \tan\alpha = \frac{\left(1.5 \cdot H_{m0} + R_{u2\%\,(\text{from 1st estimate})}\right)}{L_{Slope} - B} \tag{5.26}$$

If the run-up height or 1.5 H_{m0} comes above the crest level, then the crest level must be taken as the characteristic point above SWL.
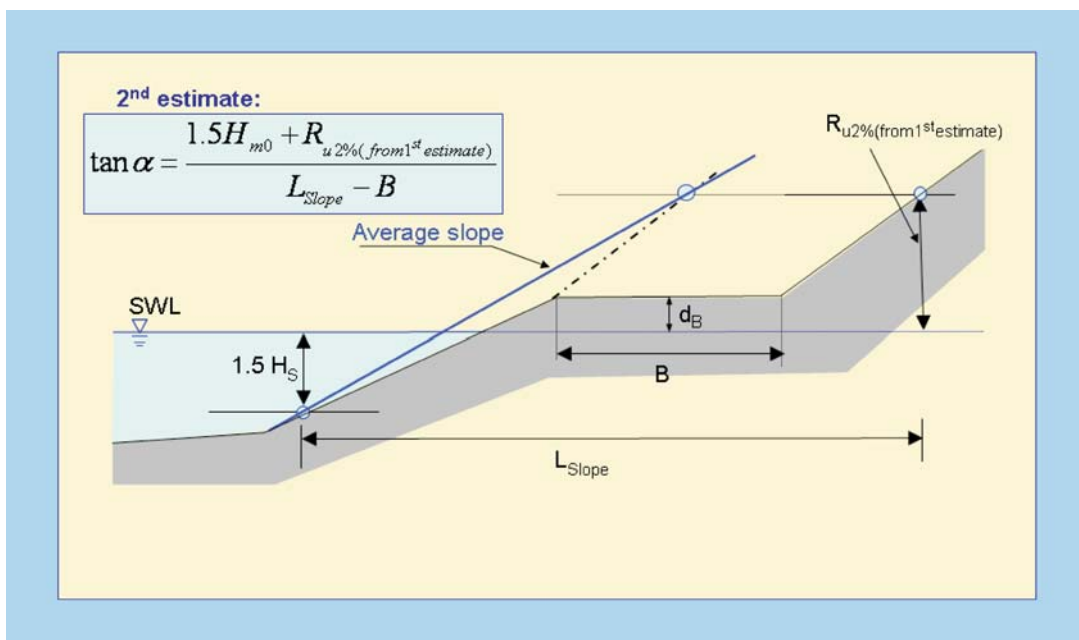

Fig. 5.26: Determination of the average slope (2nd estimate)

(b) **Influence of Berms:** A berm is a part of a dike profile in which the slope varies between horizontal and 1:15 (see Section 1.4 for a detailed definition). A berm is defined by the width of the berm B and by the vertical difference d_B between the middle of the berm and the still water level (Fig. 5.27). The width of the berm B may not be greater than $0.25 \cdot L_0$. If the berm is horizontal, the berm width B is calculated according to Fig. 5.27. The lower and the upper slope are extended to draw a horizontal berm without changing the berm height dB. The horizontal berm width is therefore shorter than the angled berm width. dB is zero if the berm lies on the still water line. The characteristic parameters of a berm are defined in Fig. 5.27.
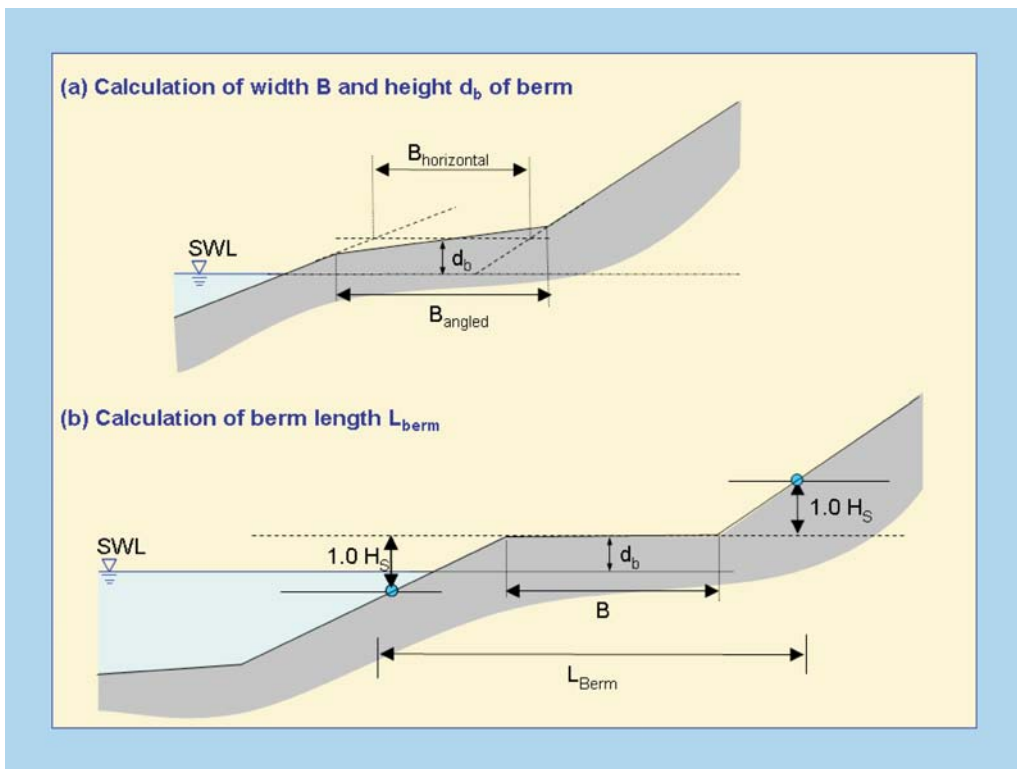

Fig. 5.27: Determination of the characteristic berm length L_{Berm}

Fig. 5.28: Typical berms (photo: SCHÜTTRUMPF)

A berm reduces wave run-up or wave overtopping. The influence factor γ_b for a berm consists of two parts.

$$\gamma_b = 1 - r_B\,(1 - r_{db}) \quad \text{for: } 0.6 \le \gamma_b \le 1.0 \tag{5.27}$$

The first part (r_B) stands for the width of the berm L_{Berm} and becomes zero if no berm is present.

$$r_B = \frac{B}{L_{Berm}} \tag{5.28}$$

The second part (r_{db}) stands for the vertical difference d_B between the still water level (SWL) and the middle of the berm and becomes zero if the berm lies on the still water line. The reduction of wave run-up or wave overtopping is maximum for a berm on the still water line and decreases with increasing d_B. Thus, a berm lying on the still water line is most effective. A berm lying below $2 \cdot H_{m0}$ or above $R_{u2\%}$ has no influence on wave run-up and wave overtopping.

Different expressions are used for r_{dB} in Europe. Here an expression using a cosine-function for r_{db} (Fig. 5.29) is recommended which is also used in PC-Overtopping.

$$r_{db} = 0.5 - 0.5\cos\left(\pi\,\frac{d_b}{R_{u2\%}}\right) \qquad \text{for a berm above still water line}$$

$$r_{db} = 0.5 - 0.5\cos\left(\pi\,\frac{d_b}{2 \cdot H_{m0}}\right) \qquad \text{for a berm below still water line} \tag{5.29}$$

$$r_{db} = 1 \text{ for berms lying outside the area of influence}$$

The maximum influence of a berm is actually always limited to $\gamma_B = 0.6$. This corresponds to an optimal berm width B on the still water line of $B = 0.4 \cdot L_{berm}$.

The definition of a berm is made for a slope smoother than 1:15 while the definition of a slope is made for slopes steeper than 1:8, see Section 1.4. If a slope or a part of the slope lies in between 1:8 and 1:15 it is required to interpolate between a bermed profile and a straight profile. For wave run-up this interpolation is written by:

$$R_{u2\%} = R_{u2\%(1:8slope)} + \left(R_{u2\%,(Berm)} - R_{u2\%,(1:8slope)}\right) \cdot \frac{(1/8 - \tan\alpha)}{(1/8 - 1/15)} \tag{5.30}$$

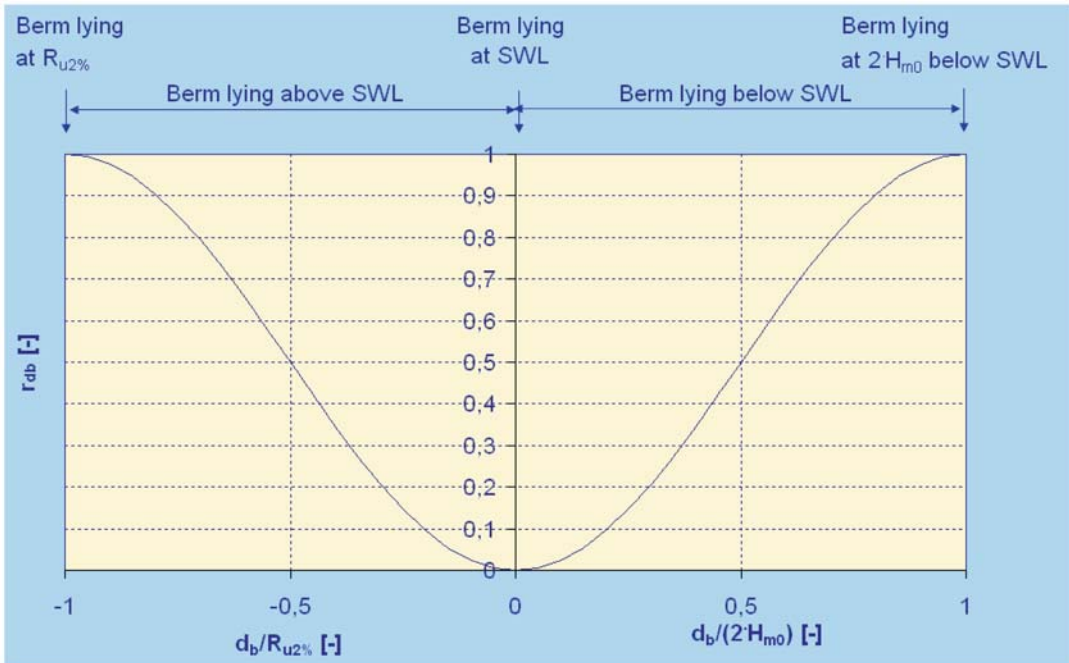A similar interpolation procedure should be followed for wave overtopping.

Fig. 5.29: Influence of the berm depth on factor r_{dh}

5.3.5 Effect of wave walls

In some cases a vertical or very steep wall is placed on the top of a slope to reduce wave overtopping. Vertical walls on top of the slope are often adopted if the available place for an extension of the basis of the structure is restricted. These are essentially relatively small walls and not large vertical structures such as caissons and quays (these are treated separately in

Fig. 5.30: Sea dike with vertical crest wall (photo: HOFSTEDE)

98

Chapter 7). The wall must form an essential part of the slope, and sometimes includes a berm or part of the crest. The effectiveness of a wave wall to reduce wave run-up and wave overtopping might be significant (Fig. 5.31).

The knowledge about the influence of vertical or steep walls on wave overtopping is quite limited and only a few model studies are available. Based on this limited information, the influence factors for a vertical or steep wall apply for the following studied application area:

- the average slope of 1.5 H_{m0} below the still water line to the foot of the wall (excluding a berm) must lie between 1:2.5 to 1:3.5.
- the width of all berms together must be no more than 3 H_{m0}.
- the foot of the wall must lie between about 1.2 H_{m0} under and above the still water line;
- the minimum height of the wall (for a high foot) is about 0.5 H_{m0}. The maximum height (for a low foot) is about 3 H_{m0}.

Fig. 5.31: Influence of a wave wall on wave overtopping (photo: SCHÜTTRUMPF)

It is possible that work will be performed to prepare guidance for wave overtopping for vertical constructions on a dike or embankment, in the future. Until then the influence factors below can be used within the application area described. Wave overtopping for a completely vertical walls is given in Chapter 7 of this manual.

For wave overtopping a breaker parameter is required, as for wave run-up. A vertical wall soon leads to a large value for the breaker parameter when determining an average slope as described in Fig. 5.25. This means that the waves will not break. The wall will be on top

of the slope, possibly even above the still water line, and the waves will break on the slope before the wall. In order to maintain a relationship between the breaker parameter and the type of breaking on the dike slope, the steep or vertical wall must be drawn as a slope 1:1 when determining the average slope. This slope starts at the foot of the vertical wall. The average slope and the influence of any berm must be determined with a 1:1 slope instead of the actual steep slope or vertical wall, according to the procedure given before.

Furthermore, the overtopping for a vertical wall on the top of a dike is smaller than for a 1:1 slope on top of a dike profile. The influence factor for a vertical wall on a slope is $\gamma_V = 0.65$. For a 1:1 slope, this influence factor is $\gamma_V = 1$. Interpolation must be performed for a wall that is steeper than 1:1 but not vertical:

$$\gamma_v = 1.35 - 0.0078 \cdot \alpha_{wall} \qquad 5.31$$

where α_{wall} is the angle of the steep slope in degrees (between 45° for a 1:1 slope and 90° for a vertical wall).

The method to calculate the reduction factor for vertical walls is very limited to the given conditions. Therefore, it is recommended to use the Neural Network for more reliable calculations.

5.4 Overtopping volumes

An average overtopping discharge does not say much about the load of the dike or revetment caused by individual waves. The significance of the individual overtopping volumes can be shown from the example in Fig. 5.32, which gives the probability distribution function of individual overtopping volumes for an average overtopping discharge of 1.7 l/s per m, a wave period of $T_{m-1,0} = 5$ s and for 7 % of overtopping waves. In this Fig. 50 % of the overtopping waves result in an overtopping volume of less than 0.06 m³ per m width but 1 % of the overtopping waves result in an overtopping volume of more than 0.77 m³ per m width, which is more than 10 times larger.

The overtopping volumes per wave can be described by a Weibull distribution with a shape factor of 0.75 and a scale factor a. It is a sharply upward bound curve in Fig. 5.32, showing that only a few very large overtopping waves count for most of the overtopping discharge. The shape factor was found to be almost constant. The scale factor a depends on the average overtopping rate q, the mean wave period T_m and the probability of overtopping waves P_{ov}. The Weibull distribution giving the exceedance probability P_V of an overtopping volume per wave V is described as:

$$P_V = P(\underline{V} \leq V) = 1 - \exp\left[-\left(\frac{V}{a}\right)^{0.75}\right] \qquad 5.32$$

with:

$$a = 0.84 \cdot T_m \cdot \frac{q}{P_{ov}} \qquad 5.33$$

If the overtopping volume per wave for a given probability of exceedance P_V is required:

$$V = a \left[- \ln \left(1 - P_V\right)\right]^{4/3} \qquad\qquad 5.34$$

For the maximum overtopping volume in a storm the following formula can be used, by filling in the number of overtopping waves N_{ov}. Note that the prediction of this maximum volume is subject to quite some uncertainty, which is always the case for a maximum in a distribution.

$$V_{max} = a \cdot \left[\ln \left(N_{ov}\right)\right]^{4/3} \qquad\qquad 5.35$$

The probability of overtopping per wave can be calculated by assuming a Rayleigh-distribution of the wave run-up heights and taking $R_{u2\%}$ as a basis :

$$P_{ov} = \exp\left[-\left(\sqrt{-\ln 0.02}\,\frac{R_C}{R_{u2\%}}\right)^2\right] \qquad\qquad 5.36$$

The probability of overtopping per wave P_{ov} is related to the number of incoming (N_w) and overtopping waves (N_{ow}) by:

$$P_{ov} = \frac{N_{ow}}{N_w} \qquad\qquad 5.37$$

Example:
The probability distribution function for wave overtopping volumes per wave is calculated for a smooth $\tan\alpha = 1{:}6$ dike with a freeboard of $R_C = 2.0$ m, a period of the incoming wave of $T_{m-1,0} = 5.0$ s and a wave height of the incoming waves of $H_{m0} = 2.0$ m. For these conditions, the wave run-up height is $R_{u2\%} = 2.43$ m, the average overtopping rate $q = 1.7$ l/(sm) and the probability of overtopping per wave is $P_{ov} = 0.071$. This means, that the scale factor a becomes $a = 0.100$. The storm duration is assumed to be 1 hour, resulting in 720 incoming waves and 51 overtopping waves. The probability of exceedance curve is given in Fig. 5.32.

5.5 Overtopping flow velocities and overtopping flow depth

Average overtopping rates are not appropriate to describe the interaction between the overtopping flow and the failure mechanisms (infiltration and erosion) of a clay dike. Therefore, research was carried out recently in small and large scale model tests to investigate the overtopping flow (see Fig. 5.33) velocities and the related flow depth on the seaward slope, the dike crest and the landward slope. Results are summarized in SCHÜTTRUMPF and VAN GENT, 2003. Empirical and theoretical functions were derived and verified by experimental data in small and large scale. These parameters are required as boundary conditions for geotechnical investigations, such as required for the analysis of erosion, infiltration and sliding.
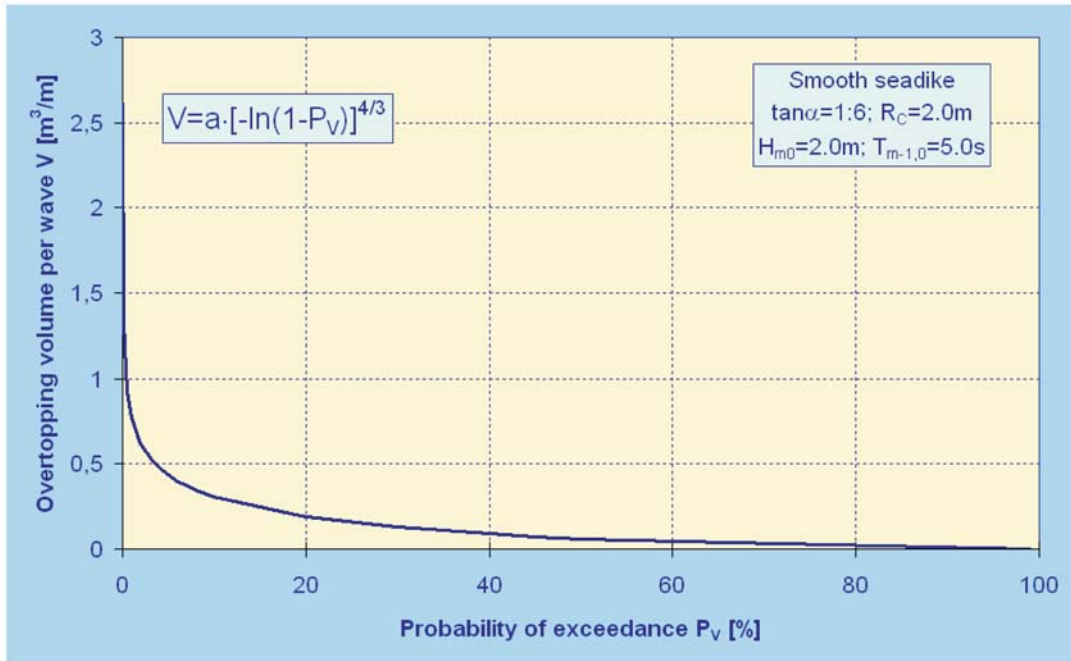
Fig. 5.32: Example probability distribution for wave overtopping volumes per wave

The parameters for overtopping flow velocities and overtopping flow depth will be described separately for the seaward slope, the dike crest and the landward slope.

Fig. 5.33: Wave overtopping on the landward side of a seadike (photo: ZITSCHER)

5.5.1 S e a w a r d S l o p e

Wave run-up velocities and related flow depths are required on the seaward slope to determine the initial flow conditions of wave overtopping at the beginning of the dike crest.

(a) Wave run-up flow depth: The flow depth of wave run-up on the seaward slope is a function of the horizontal projection x_Z of the wave run-up height $R_{u2\%}$, the position on the dike x_A and a dimensionless coefficient c_2. The flow depth of wave run-up on the seaward slope can be calculated by assuming a linear decrease of the layer thickness h_A from SWL to the highest point of wave run-up:

$$h_A(x_*) = c_2(x_z - x_A) = c_2 \cdot x_* \qquad\qquad 5.38$$

with x_* the remaining run-up length ($x_* = x_Z - x_A$) and $x_z = R_{u2\%}/\tan\alpha$.

No distinction is required here for non-breaking and breaking waves since wave breaking is considered in the calculation of the wave run-up height $R_{u2\%}$. The coefficient c_2 can be determined for different exceedance levels by Table 5.3.

Table 5.3: Characteristic values for parameter c_2 (TMA-spectra)

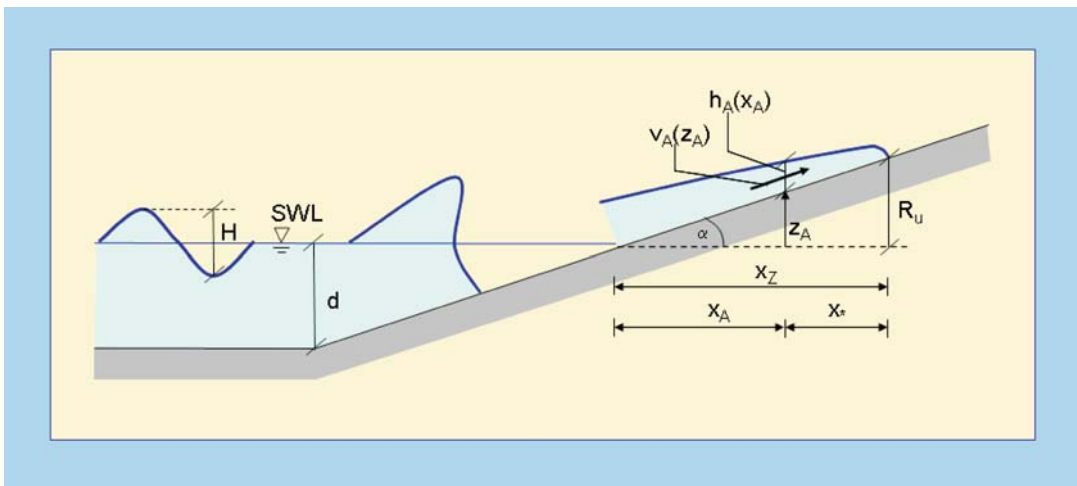| Parameter	c_2	σ'
$h_{A,50\%}$	0,028	0.15
$h_{A,10\%}$	0,042	0.18
$h_{A,2\%}$	0,055	0.22

Fig. 5.34: Definition sketch for layer thickness and wave run-up velocities on the seaward slope

(b) Wave run-up velocities: The wave run-up velocity is defined as the maximum velocity that occurs during wave run-up at any position on the seaward slope. This velocity is attributed to the front velocity of the wave run-up tongue. The wave run-up velocity can be derived from a simplified energy equation and is given by:

$$v_A = k^* \cdot \sqrt{2g\left(R_{u2\%} - z_A\right)}$$ 5.39

with v_A the wave run-up velocity at a point z_A above SWL, $R_{u2\%}$ the wave run-up height exceeded by 2 % of the incoming waves, and k^* a dimensionless coefficient.

In dimensionless form, the wave run-up velocity is:

$$\frac{v_A}{\sqrt{gH_S}} = a_0^* \sqrt{\frac{\left(R_{u2\%} - z_A\right)}{H_S}}$$ 5.40

Equation 5.40 has been calibrated by small and large scale model data resulting in values for the 2 %, 10 % and 50 % exceedance probability (Table 5.4).

Exemplarily, the decrease of wave run-up velocity and wave run-up flow depth on the seaward slope is given in Fig. 5.35.

Table 5.4: Characteristic Values for Parameter a_0^* (TMA-spectra)

Parameter	a_0^*	σ'
$v_{A,50\%}$	1.03	0.23
$v_{A,10\%}$	1.37	0.18
$v_{A,2\%}$	1.55	0.15

5.5.2 Dike Crest

The overtopping tongue arrives as a very turbulent flow at the dike crest (Fig. 5.36). The water is full of air bubbles and the flow can be called "white water flow". Maximum flow depth and overtopping velocities were measured in this overtopping phase over the crest. The overtopping flow separates slightly from the dike surface at the front edge of the crest. No flow separation occurs at the middle and at the rear edge of the crest. In the second overtopping phase, the overtopping flow has crossed the crest. Less air is in the overtopping flow but the flow itself is still very turbulent with waves in flow direction and normal to flow direction. In the third overtopping phase, a second peak arrives at the crest resulting in nearly the same flow depth as the first peak. In the fourth overtopping phase, the air has disappeared from the overtopping flow and both overtopping velocity and flow depth are decreasing. Finally, the overtopping flow nearly stops on the dike crest for small overtopping flow depths. Few air is in the overtopping water. At the end of this phase, the overtopping water on the dike crest starts flowing seaward.
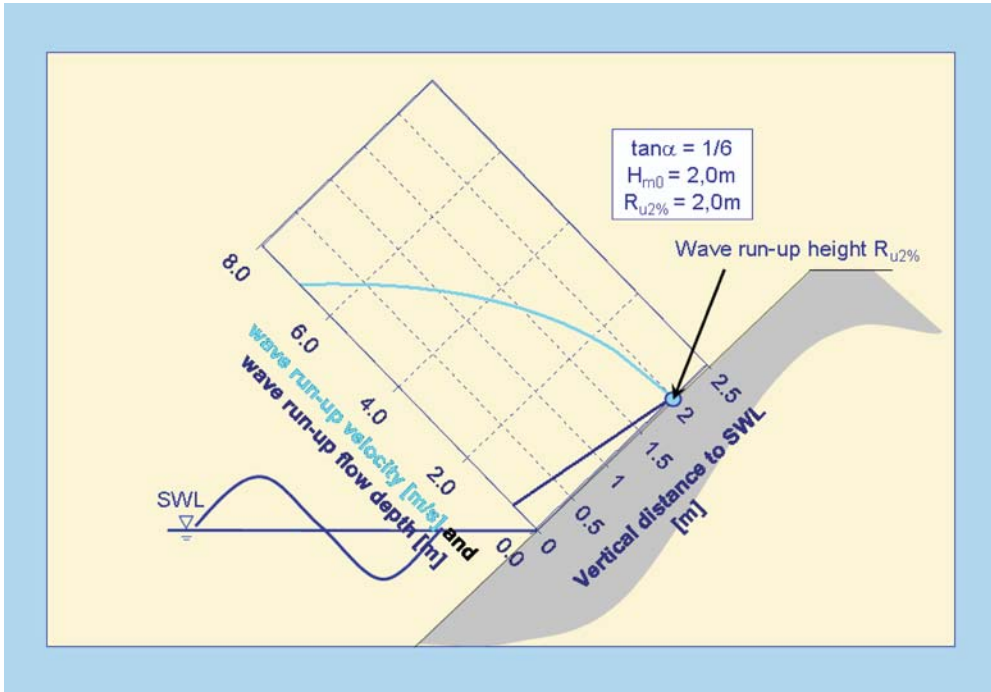
Fig. 5.35: Wave run-up velocity and wave run-up flow depth on the seaward slope (example)
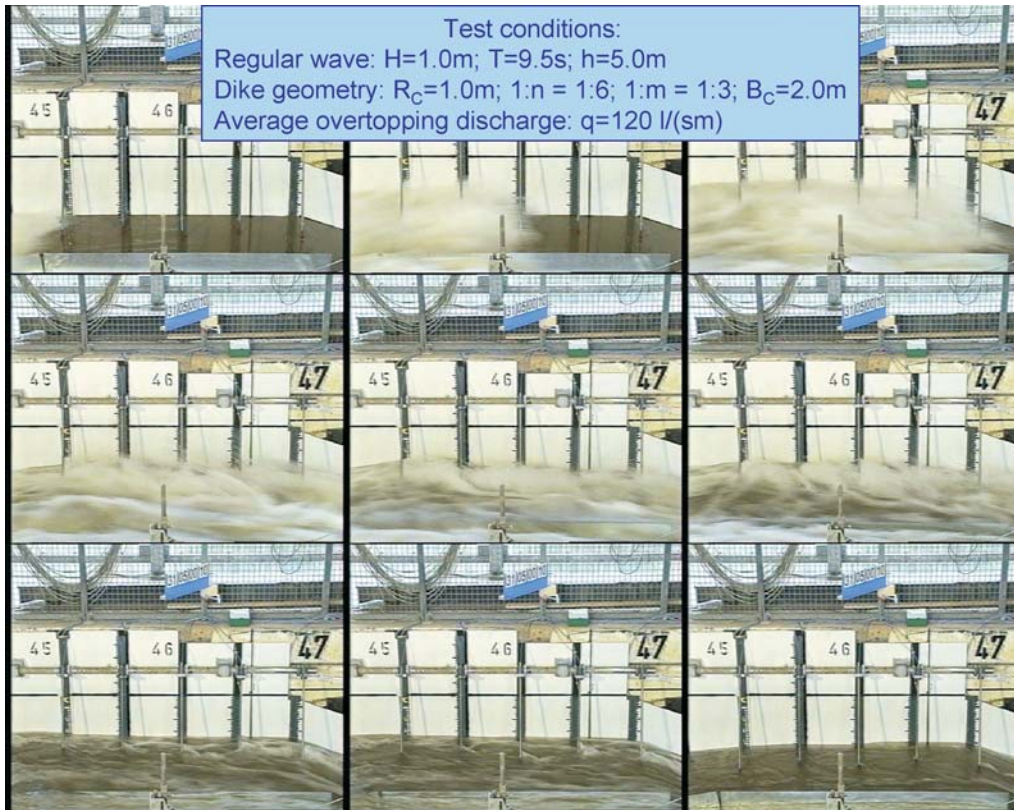

Fig. 5.36: Sequence showing the transition of overtopping flow on a dike crest
(Large Wave Flume, Hannover)

The flow parameters at the transition line between seaward slope and dike crest are the initial conditions for the overtopping flow on the dike crest. The evolution of the overtopping flow parameters on the dike crest will be described below.

(a) **Overtopping flow depth on the dike crest:** The overtopping flow depth on the dike crest depends on the width of the crest B and the co-ordinate on the crest x_C (Fig. 5.37). The overtopping flow depth on the dike crest decreases due to the fact that the overtopping water is deformed. Thus, the decrease of overtopping flow depth over the dike crest can be described by an exponential function:

$$\frac{h_C(x_C)}{h_C(x_C = 0)} = \frac{c_2(x_C)}{c_2(x_C = 0)} = \exp\left(-c_3 \frac{x_C}{B_C}\right)$$
5.41

with h_C the overtopping flow depth on the dike crest, x_C the horizontal coordinate on the dike crest with $x_C = 0$ at the beginning of the dike crest, c_3 the dimensional coefficient = 0.89 for TMA spectra ($\sigma' = 0.06$) and 1.11 for natural wave spectra ($\sigma' = 0.09$), and B_C the width of the dike crest (for $B_c = 2$ to 3 m in prototype scale).
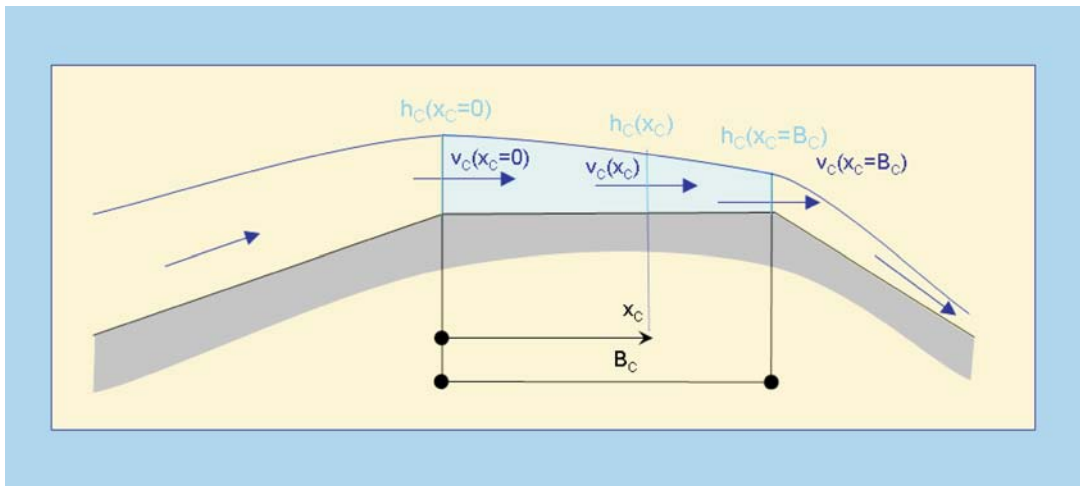

Fig. 5.37: Definition sketch for overtopping flow parameters on the dike crest

(b) **Overtopping flow velocity:** A theoretical function for overtopping flow velocities on the dike crest has been developed by using the simplified Navier-Stokes-equations and the following assumptions: the dike crest is horizontal; velocities vertical to the dike slope can be neglected; the pressure term is almost constant over the dike crest; viscous effects in flow direction are small; bottom friction is constant over the dike crest.

The following formula was derived from the Navier-Stokes-equations and verified by small and large scale model tests (Fig. 5.38):

$$v_C = v_{C(x_C=0)} \exp\left(-\frac{x_C \cdot f}{2 \cdot h_C}\right)$$
5.42

with v_C the overtopping flow velocity on the dike crest; $v_{C,(X_c=0)}$ the overtopping flow velocity at the beginning of the dike crest ($x_C = 0$); x_C the coordinate along the dike crest; f the friction coefficient; and h_C the flow depth at x_C.

From Equation 5.43 it is obvious that the overtopping flow velocity on the dike crest is mainly influenced by bottom friction. The overtopping flow velocity decreases from the beginning of the dike crest to the end of the dike crest due to bottom friction. The friction factor f was determined from model tests at straight and smooth slope to be f = 0.01. The importance of the friction factor on the overtopping flow velocities on the dike crest is obvious from Fig. 5.39. The overtopping flow velocity decreases significantly over the dike crest for increasing surface roughness. But for flow depths larger than about 0.1 m and dike crest widths around 2–3 m, the flow depth and velocity hardly change over the crest.
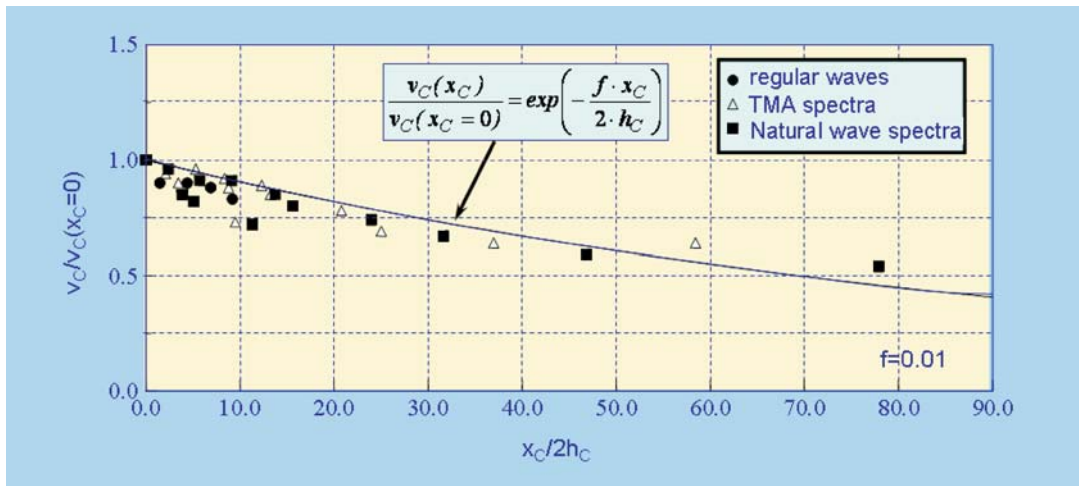

Fig. 5.38: Overtopping flow velocity data compared to the overtopping flow velocity formula
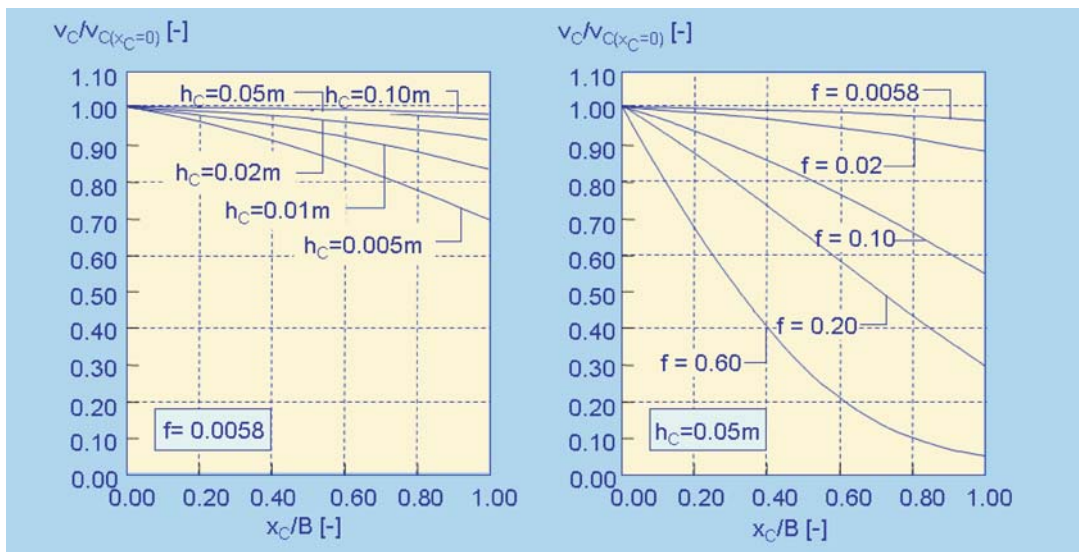

Fig. 5.39: Sensitivity analysis for the dike crest (left side: influence of overtopping flow depth on overtopping flow velocity; right side: influence of bottom friction on overtopping flow velocity)

5.5.3 Landward Slope

The overtopping water flows from the dike crest to the landward slope of the dike. The description of the overtopping process on the landward slope is very important with respect to dike failures which often occurred on the landward slope in the past. An analytical function was developed which describes overtopping flow velocities and overtopping flow depths on the landward slope as a function of the overtopping flow velocity at the end of the dike crest ($v_{b,0} = v_C(x_C = B)$), the slope angle β of the landward side and the position s_B on the landward side with $s_B = 0$ at the intersection between dike crest and landward slope. A definition sketch is given in Fig. 5.41. The following assumptions were made to derive an analytical function from the Navier-Stokes-equations: velocities vertical to the dike slope can be neglected; the pressure term is almost constant over the dike crest; and the viscous effects in flow direction are small.

Fig. 5.40: Overtopping flow on the landward slope (Large Wave Flume, Hannover)
(photo: SCHÜTTRUMPF)

This results in the following formula for overtopping flow velocities:

$$v_b = \frac{v_{b,0} + \dfrac{k_1 h_b}{f} \tanh\left(\dfrac{k_1 t}{2}\right)}{1 + \dfrac{f\, v_{b,0}}{h_b\, k_1} \tanh\left(\dfrac{k_1 t}{2}\right)}$$

5.43

with:

$$t \approx -\frac{v_{b,0}}{g \sin\beta} + \sqrt{\frac{v_b^2}{g^2 \sin^2\beta} + \frac{2 s_b}{g \sin\beta}} \quad \text{and} \quad k_1 = \sqrt{\frac{2 f\, g \sin\beta}{h_b}}$$

Equation 5.44 needs an iterative solution since the overtopping flow depth h_b and the overtopping flow velocity v_b on the landward slope are unknown. The overtopping flow depth h_b can be replaced in a first step by:

$$h_b = \frac{v_{b,0} \cdot h_{b,0}}{v_b} \qquad\qquad 5.44$$

with $v_{b,0}$ the overtopping flow velocity at the beginning of the landward slope ($v_{b,0} = v_B(s_B = 0)$); and $h_{b,0}$ the overtopping flow depth at the beginning of the landward slope ($h_{b,0} = h_B (s_B = 0)$).
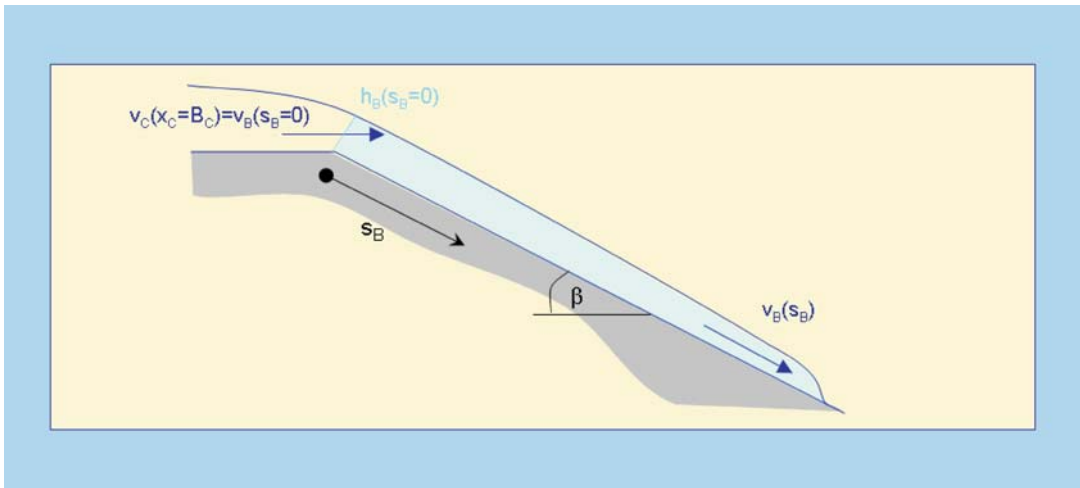

Fig. 5.41: Definition of overtopping flow parameters on the landward slope

In Fig. 5.42, the influence of the landward slope on overtopping flow velocities and overtopping flow depths is shown. The landward slope was varied between 1:m = 1:2 and 1:m = 1:6 which is in the practical range. It is obvious that overtopping flow velocities increase for steeper slopes and related overtopping flow depths decrease with increasing slope steepness.

The second important factor influencing the overtopping flow on the landward slope is the bottom friction coefficient f which has to be determined experimentally. Some references for the friction coefficient on wave run-up are given in literature (e.g. VAN GENT, 1995; CORNETT and MANSARD, 1994, SCHULZ, 1992). Here, the bottom friction coefficient was determined by comparison of the experimental to be f = 0.02 for a smooth and straight slope. These values are comparable to references in literature. VAN GENT (1995) recommends a friction coefficient f = 0.02 for smooth slopes and SCHULZ (1992) determined friction coefficients between 0.017 and 0.022.

The overtopping flow on the landward slope tends towards an asymptote for $s_b \rightarrow \infty$ which is given by:

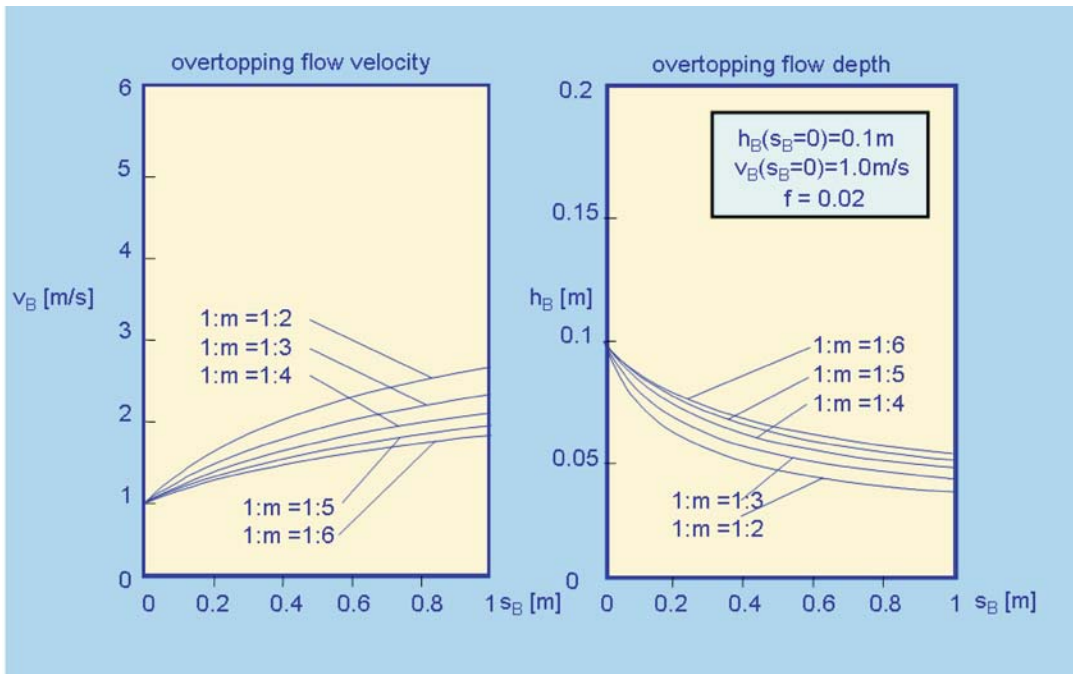$$v_b = \sqrt{\frac{2 \cdot g \cdot h_b \cdot \sin\beta}{f}} \qquad\qquad 5.45$$

Fig. 5.42: Sensitivity Analysis for Overtopping flow velocities and related overtopping flow depths
– Influence of the landward slope –

5.6 Scale effects for dikes

A couple of investigations on the influence of wind and scale effects are available for sloping structures all of which are valid only for rough structures. Sea dikes are generally smooth and covered e.g. by grass, revetment stones or asphalt which all have roughness coefficients larger than $\gamma_f = 0.9$. Hence, there are no significant scale effects for these roughness coefficients. This is however only true if the model requirements as given in Table 4.3 in Section 4.8.3 are respected.

For rough slopes as they e.g. occur for any roughness elements on the seaward slope, scale effects for low overtopping rates cannot be excluded and therefore, the procedure as given in Section 6.3.6 should be applied.

5.7 Uncertainties

In section 5.3.1 model uncertainties have been introduced in the calculation by defining the parameter b in Equation 5.8 as normally distributed parameter with a mean of 4.75 and a standard deviation of $\sigma = 0.5$ for breaking waves and $b = 0.2$ and $\sigma = 0.35$ for non breaking waves. This has also been illustrated by Fig. 5.6 and Fig. 5.7, respectively, showing the 90 % confidence interval resulting from these considerations.

In using the approach as proposed in section 4.8.1, a model uncertainty of about 60 % is obtained. Note that this approach comprises a model factor for Equation 5.8 in total rather than the uncertainty of the parameter b only as used in Fig. 5.6 and Fig. 5.7. The latter approach comprise various uncertainties from model tests, incl. repeatability of tests, model

effects, uncertainties in wave measurements, etc. whereas the following uncertainties for the assessment of the wave heights, the wave period, the water depth, the wave attack angle, constructional parameters such as the crest height and the slope angle are not included.

The uncertainties of these parameters may be estimated following an analysis of expert opinions from SCHÜTTRUMPF et al. (2006) using coefficients of variations (CoV) for the wave height H_{m0} (3.6 %), the wave period (4.0 %), and the slope angle (2.0 %). Other parameters are independent of their mean values so that standard deviations can be used for the water depth (0.1 m), the crest height and the height of the berm (0.06 m), and the friction factor (0.05). It should be noted that these uncertainties should only be used if no better information (e.g. measurements of waves) are obtainable.

Using these values together with the already proposed model uncertainties for the parameter b in Equation 5.8, crude Monte Carlo simulations were performed to obtain the uncertainty in the resulting mean overtopping discharges. Plots of these results are shown in Fig. 5.43.
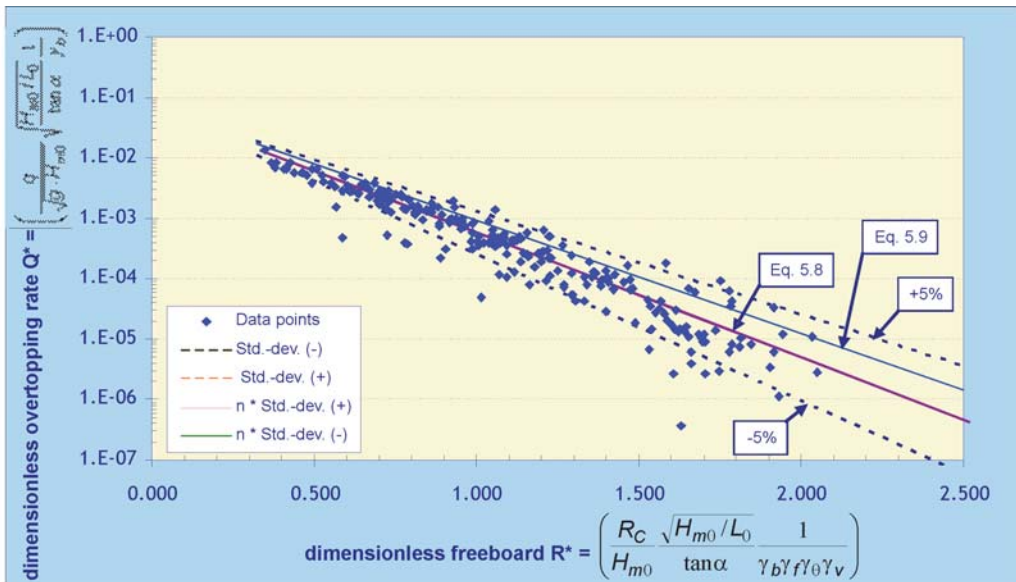

Fig. 5.43: Wave overtopping over sea dikes, including results from uncertainty calculations

As compared to Fig. 5.6 and Fig. 5.7, respectively, it can be seen that the resulting curves (denominated as 'n*std.-dev.' in Fig. 5.43) are only giving slightly larger uncertainty bands as the 5% lines resulting from calculations with model uncertainties. This suggests a very large influence of the model uncertainties so that no other uncertainties, if assumed to be in the range as given above, need to be considered. It is therefore proposed to use Equations 5.8 and 5.9 as suggested in section 5.3.1. In case of deterministic calculations, Equation 5.9 should be used with no further adaptation of parameters. In case of probabilistic calculations, Equation 5.8 should be used and uncertainties of all input parameters should be considered in addition to the model uncertainties. If detailed information of some of these parameters is not available, the uncertainties as proposed above may be used.

It should be noted that only uncertainties for mean wave overtopping rates are considered here. Other methods such as flow velocities and flow depths were not considered here but can be dealt with using the principal procedure as discussed in section 1.5.4.